2011

Computational Modeling Of Low Velocity Impact Loading Of Composite With And Without Electrospun Nanofiber

Abu Hasnath Rasel
North Carolina Agricultural and Technical State University

COMPUTATIONAL MODELING OF LOW VELOCITY IMPACT LOADING OF COMPOSITE WITH AND WITHOUT ELECTROSPUN NANOFIBER

by

Abu Hasnath Rasel

A dissertation submitted to the graduate faculty
in partial fulfillment of the requirements for the degree of
MASTER OF SCIENCE

Department: Computational Science and Engineering
Major: Computational Science and Engineering
Major Professor: Dr. Ajit Kelkar

North Carolina A&T State University
Greensboro, North Carolina
2011

School of Graduate Studies
North Carolina Agricultural and Technical State University

This is to certify that the Master's Thesis of

Abu Hasnath Rasel

has met the thesis requirements of
North Carolina Agricultural and Technical State University

Greensboro, North Carolina
2011

Approved by:

_____	_____
Dr. Ajit Kelkar Major Professor	Dr. Ram Mohan Committee Member
_____	_____
Dr. S. N. Patankar Committee Member	Dr. M. U. Bikdash Department Chairperson

_____
Dr. Sanjiv Sarin
Interim Associate Vice Chancellor
for Research and Dean of Graduate Studies

DEDICATION

I dedicate this work to my parents, brothers and sister and my nephew Naufil, niece Sanjida and Rumaysa. Without their support, this work would not have been possible.

BIOGRAPHICAL SKETCH

Abu Hasnath Rasel was born on November 1, 1983 in Dhaka, Bangladesh. He received his Bachelor of Science in Mechanical Engineering from Bangladesh University of Engineering and Technology in 2006. He received his Master of Engineering in Mechanical Engineering from the Illinois Institute of Technology, Chicago, IL in 2009.

He joined North Carolina Agricultural and Technical State University, Greensboro, NC in 2009 to pursue Master of Science in Computational Science and Engineering. He worked as an Engineering Intern at Fresh Express (2008), Illinois and bioMerieux (2010), North Carolina.

ACKNOWLEDGEMENTS

I would like to express my profound gratitude to my advisor, Dr. Ajit Kelkar, for his continuous support and guidance throughout my work at North Carolina Agricultural and Technical State University, Greensboro, NC. I am really grateful to him for giving me the opportunity to learn about computational study and manufacturing processes of composites.

I would also like to thank Dr. Ram Mohan, for serving my thesis committee and providing his encouragement and guidance throughout graduate studies. My special thanks to Mr. Riba and Dr. Ronnie Bolick for teaching me the manufacturing and testing processes of composites.

I am grateful to Ms. Lydia Leak of CSE Department at North Carolina Agricultural and Technical State University for her wonderful support.

TABLE OF CONTENTS

LIST OF FIGURES

FIGURES **PAGE**

FIGURES **PAGE**

FIGURES **PAGE**

FIGURES **PAGE**

LIST OF TABLES

TABLES **PAGE**

ABSTRACT

Rasel, Abu Hasnath. COMPUTATIONAL MODELING OF LOW VELOCITY IMPACT LOADING OF COMPOSITE WITH AND WITHOUT ELECTROSPUN NANOFIBER**. (Advisor: Dr. Ajit Kelkar),** North Carolina Agricultural and Technical State University.

The objective of this work is the computational study of composite laminates under high velocity impact loadings. Even with the blessings of modern technology, manufacturing and testing of composites do not always seem to be cost effective. To keep pace with the fast moving global market, a new tool is absolutely necessary that can give reliable results quickly. Over the last decades computational study became a strong and effective tool for the researchers for testing composite materials in a virtual world. The virtual model and the material system of the test specimen can be built in a computer using different modeling software. Finite element analysis is the powerful numerical technique which can be used to predict the behavior of the test specimen under impact loading without incurring the cost and time associated with manufacturing and testing the test specimens. The present study includes analytical investigation of the high velocity impact behavior of ten (10) EG layer woven laminates with and without electrospun nanofibers using LS-DYNA. It was observed that composites with nanofibers in between layers perform better in low velocity impact resistance compared to composites without nanofibers.

CHAPTER 1

INTRODUCTION AND PREVIEW

1.1 Motivation for Research

In the past, many aircraft accident happened because of the impact of different kinds of birds with aircraft. The Federal Aviation Administration estimates the problem costs US aviation 600 million dollars annually and has resulted in over 200 worldwide deaths since 1988 [1]. In the United Kingdom, the Central Science Laboratory estimates that worldwide, the cost of bird strikes to airlines is around US$1.2 billion annually. The first fatal strike was recorded in 1912 when aero-pioneer Cal Rodgers collided with a gull which became jammed in his aircraft control cables. Between the years 1912 to 1995,231 people died in almost 42 accidents [1]. It has been found from statistical analysis that 77% of the accidents to the airliners are caused by engine ingestions which happens due to flocks of birds and 23% of the accidents happen due to bird impacting the air wing or the windshield of the airplane or helicopter. Bird impacts are considered as a serious safety and economic hazard for the airplane industry. Laminated composites can be used to replace the traditional aluminum alloy wing structures to withstand such impact loads. In the present study, an attempt has been made to simulate the impact behavior of laminated composite with and without electrospinning under low velocity impact condition using a finite element approach. Figures 1.1, 1.2, 1.3, 1.4 and 1.5 show airplane and helicopter damage.

Figure 1.1. View of fan blades of JT8D jet engine after a bird strike [2]

Figure 1.2. F-16 canopy after a bird strike [3]

Figure 1.3. A hawk stuck in the nosecone of a C-130 [4]

Figure 1.4. A UH-60 Black Hawk after a collision with a common crane, and the resulting failure of the windshield [5]

1.2 Composites

Composites are combinations of two or more materials embedded in another material called matrix. The combination offers properties which are superior to individual component properties. Composites are known for their high weight specific mechanical properties and are therefore used in numerous lightweight engineering applications. Their high strength to weight ratio, high creep resistance, high tensile strength and high toughness are the major reasons behind the use of composites in different applications. These materials are used not only in aircraft industry, but in civil, mechanical and other areas.

The three types of composites are:

1. Particle-reinforced composites (Figure 1.5)
2. Fiber-reinforced composites (Figure 1.6)
3. Structural composite (Figure 1.7)

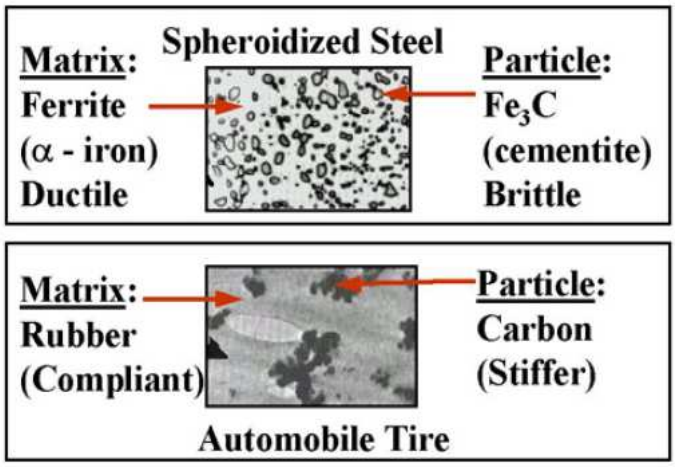

Figure 1.5. Example of particle reinforced composites [6]

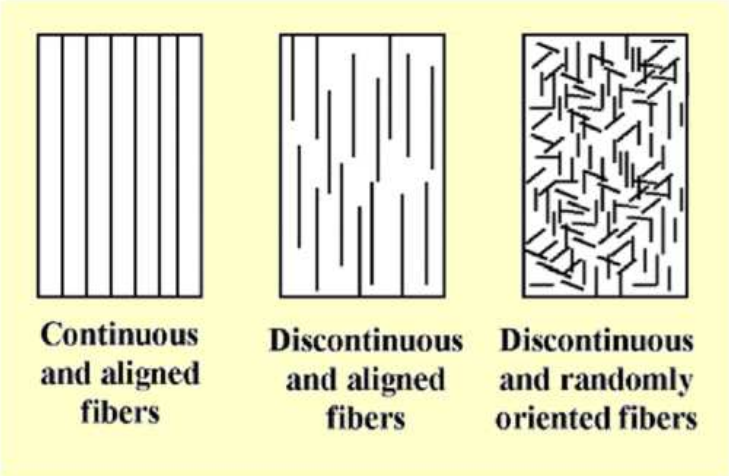

Figure 1.6. Fiber orientation in fiber reinforced composites [7]

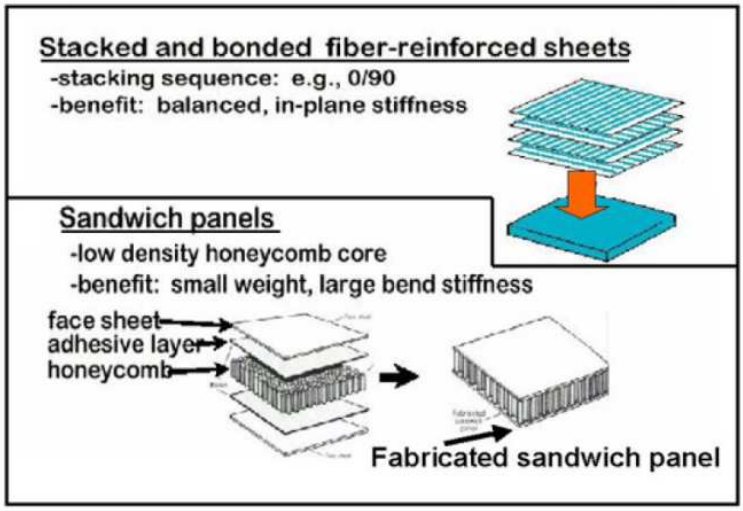

Figure 1.7. Structural composites [8]

1.3 Electrospinning

For the last couple of decade electrospinning has become a suitable process to produce uniform diameter nanofibers from different polymers, ceramics, metals and their composites. Nanofibers from variety of polymers and ceramics with porous, flat and hollow cross sections produced by electrospinning are mainly used for applications such as composite reinforcement, filters, sensors for protective clothing, and diverse biomedical applications. In the present study Tetra Ethyl Ortho Silicate (TEOS) electrospun nanofibers are used to reinforce fiber glass composites. These nanofibers resist delamination of the composite during impact loading.

The Figure 1.8 shows the general schematic diagram of an electrospinning setup. In the electrospinning process, a solution droplet is fed to the spinneret tip at a controlled

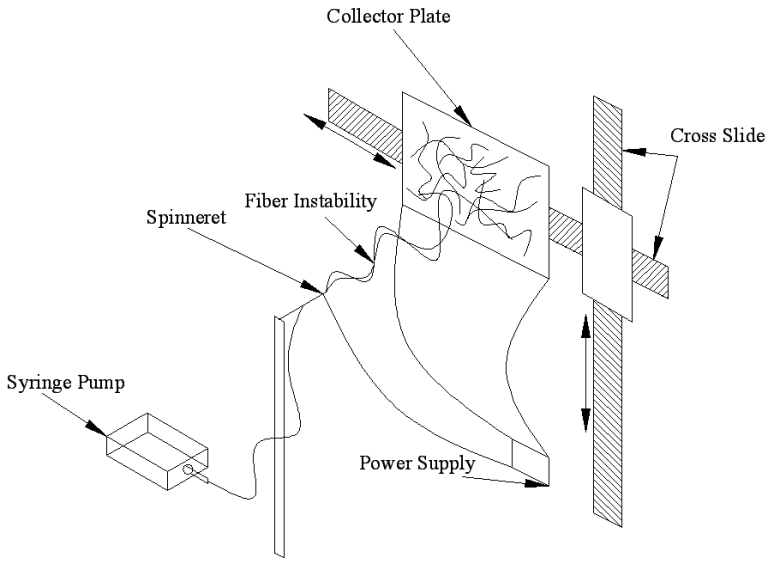

Figure 1.8. Schematic of electrospinning setup [8]

rate using a programmable dispensing pump. The solution droplet at the tip of the spinneret is acted upon by electro-hydrodynamic forces. Due to the potential difference applied between spinneret and collector plate the solution droplet experiences an electrical force. The spinneret is kept at a positive potential and the collector plate is generally kept grounded. Due to this applied potential difference, the solution droplet at the tip of the spinneret acquires positive charge on the surface. Due to the surface tension of the liquid solution the solution droplet experiences a hydrodynamic force. This solution droplet gets attracted towards the collector and forms a 45^0 semi-angle at the tip known as "Taylor Cone" [7]. If the viscosity of solution is sufficient to provide stringiness, there is elongation of the droplet into a jet which forms a fiber in the range of 3 nanometer to 1 micrometer depending on the solution's properties.

Due to their important properties like highly diverse material compatibility and high surface area to volume ratio, consistent porosity electrospun nanofibers can be used in different areas. Currently the possibilities of using electrospun nanofibers in the following fields are being explored. Figure 1.9 shows application of electrospun nanofibers in different areas. Using nanofibers in composites may increase different material properties.

1.4 Research Outline and Objectives

This study involves modeling and simulation of impact behavior of ten ply E-glass fiber composite with and without TEOS electrospun nanofibers. The simulation is

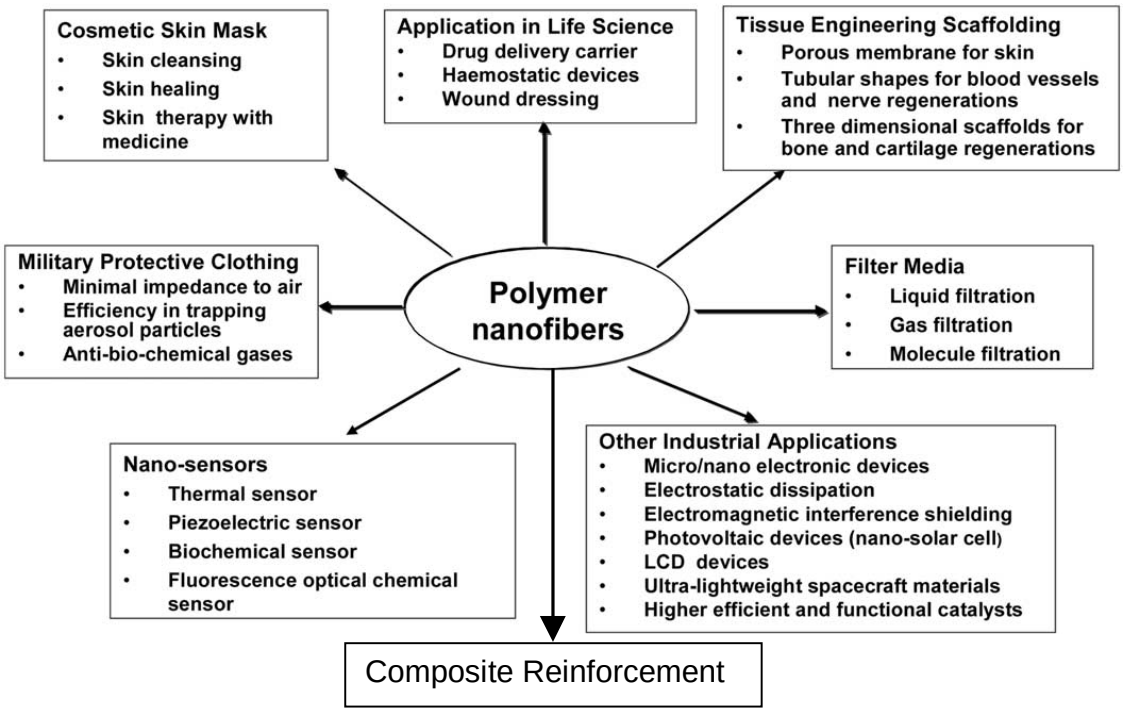

Figure 1.9. Fields of applications of electrospun nanofibers [8]

using the finite element method. One of the main objectives of the simulation is to avoid expensive fabrication of composites and experiment time. This research work consists of finite element modeling using VPG 3.1(Virtual Proving Ground). VPG is used as a preprocessor, time dependent computation using the transient dynamic finite element program LSDYNA and post processing using LSPREPOST. In this research work the composite plates are modeled with and without TEOS electrospun nanofibers. The effects of low velocity impact loading on each type of composite plate were studied.

1.5 Literature Review

In last few decades numerous experiments and much research have been done to understand and simulate the behavior of composites under low velocity impact loading. Rotem et al. [9], Lifdhitz et al. [10] and Sierakowski et al. [11] made the first attempt to characterize composite materials under dynamic loading. Sankar et al.[12] provided semi-empirical formula to predict impact characteristics like peak force, contact duration and peak strain on rear surface. Wang et al. [13] performed the experiments on 3d woven Blast/Aramid hybrid composite under low velocity impact to understand the effect on the properties of composites. Sarah et al. [14] studied the structural response of impact-damaged composite panel through different experiments. Vijay et al. [15] modeled woven roving glass, stitch bonded glass and stitched bonded carbon composites subjected to low velocity impact loads and evaluated performance of the materials.

In addition to experimental investigations the result of numerous studies are available in the literature which involve a numerical simulation approach. In 1978 Sedgwick performed a series of impact and penetration simulations using the HELP 2-dimensional Eulerian continuum mechanics code. In 1984, Jonas et al. [16] conducted a simulation of impact between a rigid surface and a thin elastic plate using Dyna-3D. Lee and Sun et al. [17] studied the dynamic penetration of Carbon Fiber Reinforced Plastic (CFRP) laminates experimentally with a flat ended cylindrical projectile. They concluded that the penetration process can be divided into three different stages: pre-delamination (fiber crushing), post-delamination before plugging and post plugging. Mines et al. [18] performed experiments on transverse impacts of E-glass/polyester laminates of different

thickness with different projectile shape. He concluded that the energy absorption mechanisms during penetration and perforation showed the same behavior explained by Lee and Sun et al. [17].

In the past many scientists and engineers have used LSDYNA to simulate complex physical problems. Xiahua et al. [19] used LSDYNA to predict the behavior of polymer matrix composite under high strain rate impact. Bhuson et al. [20] performed low velocity impact loading on hybrid composites using LSDYNA. He validated the simulation results with experimental results. Alastair et al. [21] performed simulation of impact damage in double walled sandwich composite structures by incorporating both composite ply damage model and inter-ply delamination models in commercially available explicit finite element codes. Ipson et al. [22] performed experiments on resistance of a barrier on to ballistic penetration. He used statistical sampling method in his simulations.

In the present study, a finite element based approach has been used to model two ten layer composite laminate configurations using VPG 3.1.1 preprocessor. Two different composite configuration 10 EG without electrospun nanofibers and 10EG with electrospun nanofibers were studied. The subsequent chapters present the computational modeling and simulation of composites.

CHAPTER 2

COMPUTATIONAL MODELING AND SIMULATION

2.1 Need for Computer Simulation for Low Velocity Impact

Computer simulation for impact loading analysis has contributed greatly to shortening the development period for composites with its advantages in numerical simulation techniques and computational capabilities. The main purpose of impact analysis is to evaluate the structural performance under different velocities in the early stages of composite design. FEA has been proven to be a powerful tool in analyzing various physical phenomena and a valuable aid to support in early stage of design process. Codes such as LSDYNA-3d are used to perform realistic and predictive impact simulation. The FEA codes are three-dimensional, nonlinear and are used for analyzing the large deformation dynamic response of elastic and inelastic structures with the use of explicit time integration schemes.

Developing composites for specific applications such as impact resistance materials has been one of the challenges for engineers. Composites can be designed with different configurations for different applications. It is really expensive and time consuming to develop composites and perform impact analysis experimentally. It takes two to four days to make one sheet of electrospun nanofibers. It takes more than a day to develop composite panels. To keep pace with the fast growing global market it is not economically viable to take the time to make composites with different design configuration and perform the experiments. With the improvements in computer

technology and software it is now possible to perform complex and long calculations using high performance computers. A virtual model of the composite can be built using one of the different preprocessing softwares such as VPG and the finite element analysis can be performed using one of different commercially available codes such as LSDYNA. In the present study ten ply E-glass composites with and without nanofibers are modeled using VPG 3.1.1. The materials properties, contact surfaces and boundary conditions are provided based on actual physical experiments.

2.2 LS-DYNA

LS-DYNA is a multi-purpose, explicit and implicit finite element program, developed by Livermore Software Technology Corporation, California that is used to analyze the nonlinear dynamic response of structures. Its has fully automated contact analysis capability and a wide range of constitutive models to simulate different engineering materials (any isotropic material, orthotropic, elastic, elasto-plastic etc.). It has the high scalability that has enabled users worldwide to solve effectively many complex problems.

LS-DYNA has many features that can be used to simulate the physical behavior of 2D and 3D structures: nonlinear dynamics, thermal, failure, contact, quasi-static, Eulerian, Arbitrary-Lagrangian-Eulerian (ALE), Fluid-Structure-Interaction (FSI), multi-physics coupling, biomedical applications, fracture applications etc. LS-DYNA is mostly well-known for crashworthiness analysis and sheet metal forming analysis. In addition to all these applications LS-DYNA is extensively used to simulate impacts on structures from drop tests, underwater shock, explosions or high-velocity impacts. Explosive

forming, process engineering, accident reconstruction, vehicle dynamics, thermal brake disc analysis or nuclear safety are some of the areas where LS-DYNA is being used. In cutting-edge research LS-DYNA is used to investigate the behavior of materials like composites, ceramics, concrete, or wood. Moreover, it is used in modeling in the field as diverse as biomechanics, human modeling, molecular structures, casting, forging, or virtual testing.

LS-DYNA runs on a variety of platforms, including Intel based PC's (Windows, Linux), UNIX workstations, supercomputers, and massively parallel computers. The code is fully compatible with parallel computing where multiple processors are used. In addition, domain decomposition is available. Parts of a job can be distributed to several machines with separate processors and memories (MPP). The main benefit of MPP is better performance in terms of CPU timing and scalability, when several CPU's are used.

LS-DYNA is an appropriate choice to investigate phenomena that involve large deformations, sophisticated material models and complex contact conditions. LS-DYNA allows running an analysis explicitly or implicitly and combining different disciplines such as coupled thermal analysis, fluid dynamics, fluid-structure interaction, SPH (Smooth Particle Hydrodynamics), EFG (Element Free Galerkin). For many products LS-DYNA is an essential tool to reduce the time to market. LS-DYNA assists design of robust products. With the option of multidisciplinary simulations LS-DYNA significantly increases the potential for developing innovative products with reduced time and expense.

2.3 Lagrangian Approach

In a Lagrangian coordinate system the coordinates move with the material, making it suitable to follow the regions of relatively low distortions and possibly large deformations. The Lagrangian coordinate system will deform with material and therefore accurately define material interfaces as shown in Figure 2.1 below. The history of the state of the material in the cell is known completely. Compared to the Eulerian method the Lagrangian method tends to be faster computationally as no transport of material through the mesh needs to be calculated which saves time. The main disadvantage of Lagrangian formulation is excessive distortion leads to much smaller time steps. To overcome this disadvantage proper element deletion criteria should be used.

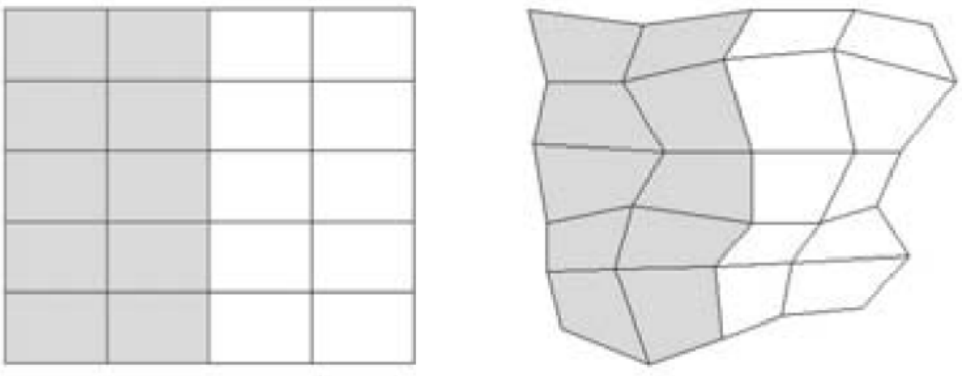

Figure 2.1. Undeformed and deformed shading in lagrangian coordinate systems, different colors represents different materials

Other popular methods of formulation are Eulerian, Discrete Lagrangian formulation and smooth particle hydrodynamics. Eulerian meshes are stable because they can sustain large deformation and they also allow flow calculation. But this formulation needs a very fine mesh and computational cost is high. The computation cost is high for the discrete element method. The final state of the failed element can not be known using a smooth particle hydrodynamic approach. Based on all the pros and cons of different methods, it can be concluded that Lagrangian formulation with effective plastic strain can be the best choice with least computation cost for studying low velocity impact.

The Lagrangian formulation, as described in the LS-DYNA [23] theory manual, considers a body, as shown in Figure 2.2, that moves from state A to state B in time t with a deformed shape,

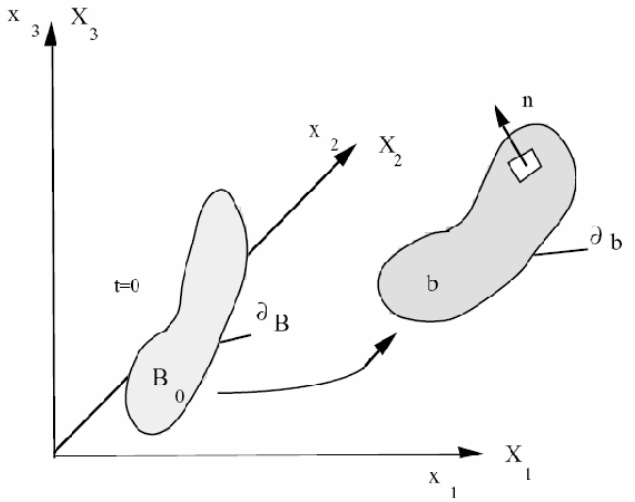

Figure 2.2. Lagrange formulation

The displacement vector at any time t is given as,

$$x_t = x_t(X_\alpha, t)$$

Here, at t=0, the initial conditions, the displacement and the velocity are respectively,

$$x_t(X_\alpha, 0) = X_\alpha$$

$$\dot{x}_t(X_\alpha, 0) = V_t(X_\alpha)$$

The momentum equation is can be expressed as,

$$\sum_{m=1}^{n} \left\{ \int_{v_m} \rho N^t N a \, dv + \int_{v_m} B^t \sigma \, dv - \int_{v_m} \rho N^t b \, dv - \int_{\partial b_1} N^t t \, ds \right\}^m = 0$$

Here, N is an Interpolation matrix, σ is the stress vector, B is the strain displacement matrix, a is the nodal acceleration vector, b is the body force load vector and t are applied traction loads.

The stress vector, σ can be defined as,

$$\sigma^t = (\sigma_{xx}, \sigma_{yy}, \sigma_{zz}, \sigma_{xy}, \sigma_{yz}, \sigma_{zx})$$

The nodal acceleration vector, a can be defined as,

$$\begin{bmatrix} \ddot{x}_1 \\ \ddot{x}_2 \\ \ddot{x}_3 \end{bmatrix} = \mathrm{N} \begin{bmatrix} a_{x_1} \\ a_{y_1} \\ \vdots \\ a_{y_k} \\ a_{z_k} \end{bmatrix} = \mathrm{N}\, a$$

The body force load vector, b and applied traction forces are,

$$b = \begin{bmatrix} f_x \\ f_y \\ f_z \end{bmatrix}, \quad t = \begin{bmatrix} t_x \\ t_y \\ t_z \end{bmatrix}$$

2.4 VPG

Virtual Proving Ground (eta/VPG) is a fully integrated, dynamic, nonlinear, finite element software package, developed by Engineering Technology Associates Inc., used to create, analyze, edit, and visualize dynamic, nonlinear engineering problems. Using VPG, engineers all over the world are reducing product development costs and improving product quality and safety. Using VPG, engineers are able to do this at a fraction of the cost of using competitive products. VPG provides an efficient and comprehensive environment for development of finite element models. VPG delivers a unique set of tools which allow researchers to create and visualize advanced simulations for different complex engineering problems. The software includes an integrated preprocessor, post processor, and solver. VPG is a complete CAE software toolset for applying theory and

engineering principles common in areas of mechanical and structural engineering. VPG provides a single package for use in analysis of multi-body dynamics problems, linear static, nonlinear static, and dynamic nonlinear finite element analysis.

VPG allows users to create complete simulations from the graphical user interface. It can create model files compatible with LS-DYNA, NASTRAN, RADIOSS etc. VPG can also import CAD data from different commercial solid modeling softwares such as Pro/Engineer, Solidworks, Catia etc.

VPG enables users to create system level simulations of mechanical systems such as vehicle suspensions, bearings, joints and linkages. VPG enables users to drfine components such as flexible bodies, combining the traditional kinematic/dynamic simulation methods with finite element analysis methods. The results are simulations that provide greater insight and opportunities to improve design. VPG Drop Test has complete dummy library, barrier library and airbag folding system. These enable users to set-up complex simulations for standard vehicle impact simulations. VPG users can quickly and reliably create simulation models that previously took a great deal of expertise and time to create. VPG Safety Module Features include Suspension Library, Parametric Tire Modeler, Road Surface Library, Fatigue Calculation and Post Processing, Dummy Library, Airbag Folder and Drop Test Module for Electronics/Packaging.

2.5 Modeling and Property Evaluation

The virtual model of the E-Glass laminate is built based on original E-Glass laminate. The actual E-glass laminate is shown in Figure 2.3. The model of composite

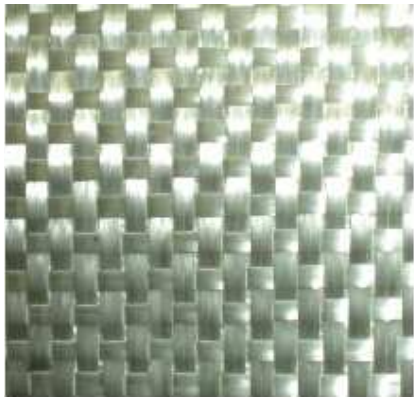

Figure 2.3. E-glass actual laminate

layers is built using a mosaic fashion [24] as shown in Figure 2.4. The layer is fully developed using repeating unit. The repeating unit is the smallest unit. This smallest unit is repeated in the whole system in x-y plane. The warf (0 degree) and the weft (90 degree) of composite are represented by the unit cell. The unit cell is developed using 8-node solid elements. In a unit cell, the warf (0 degree) and the weft (90 degree) are defined as orthotropic materials. Figure 2.5 shows the cross-section of a ten layer composite model without nanofibers. Figure 2.6 shows the cross section of a ten layer composite model with nanofibers. The nanofibers are placed in between the layers. The thickness of each fiberglass layer is 0.09 inch. The total thickness of composite without nanofibers is 0.9 inch. The thickness of each layer of nanofibers is .002. The total thickness of composite with nanofibers is 0.108 inch. Figure 2.7 shows the complete model.

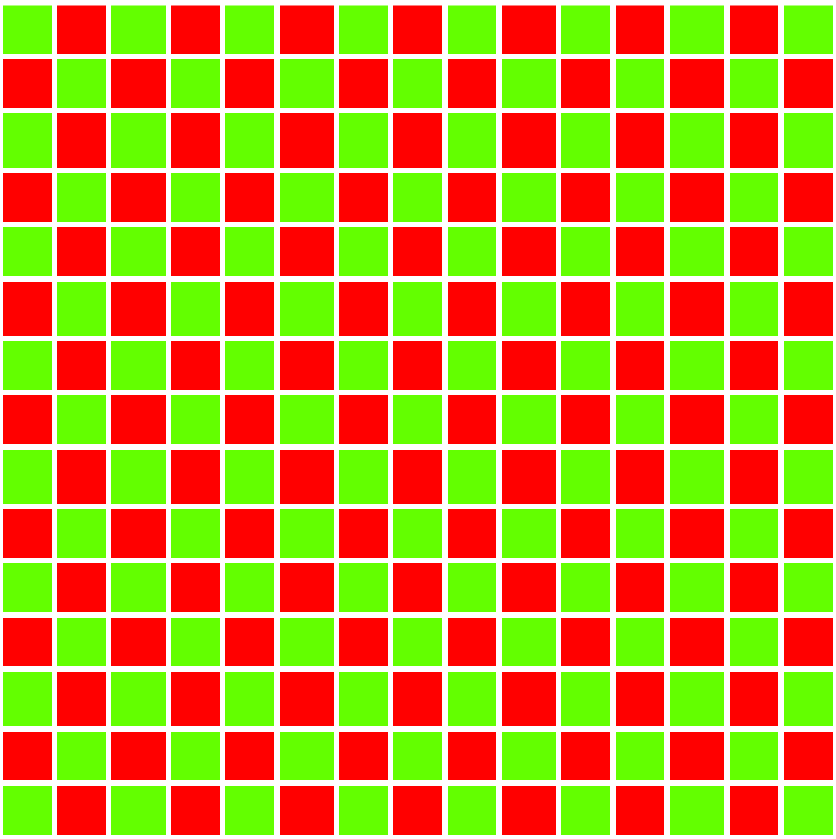

Figure 2.4. E-glass model laminate

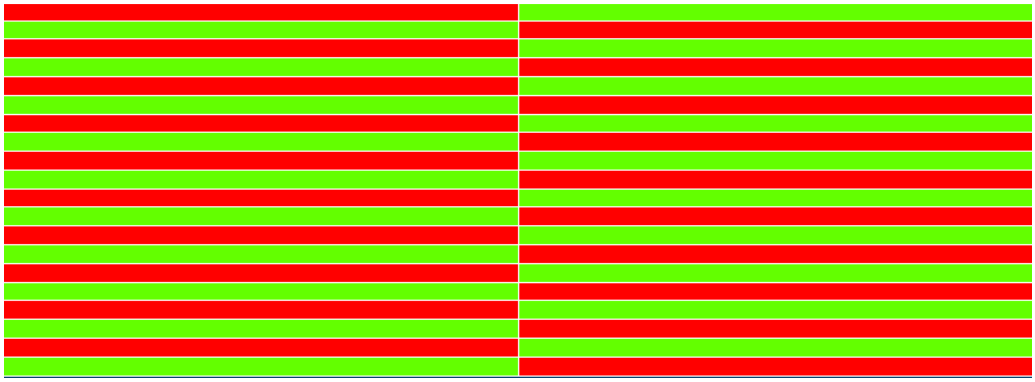

Figure 2.5. Cross section without nanofiber

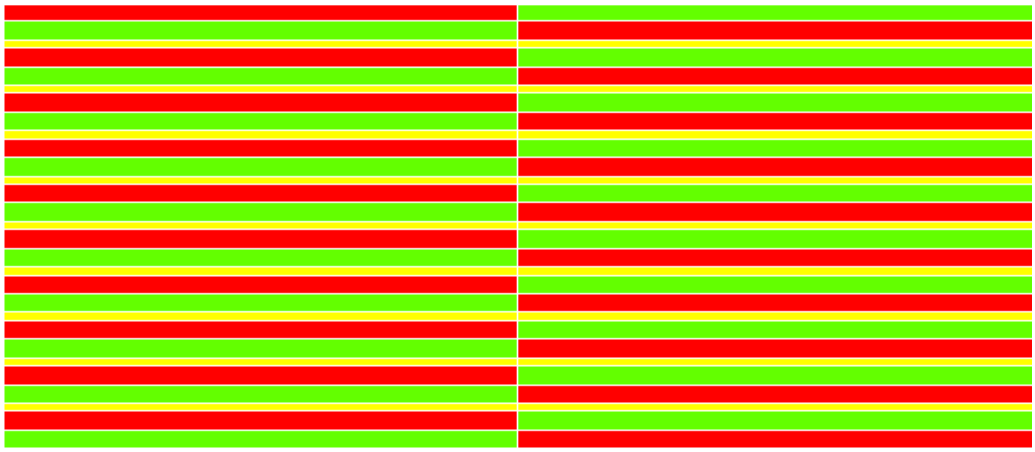

Figure 2.6. Cross section with nanofiber

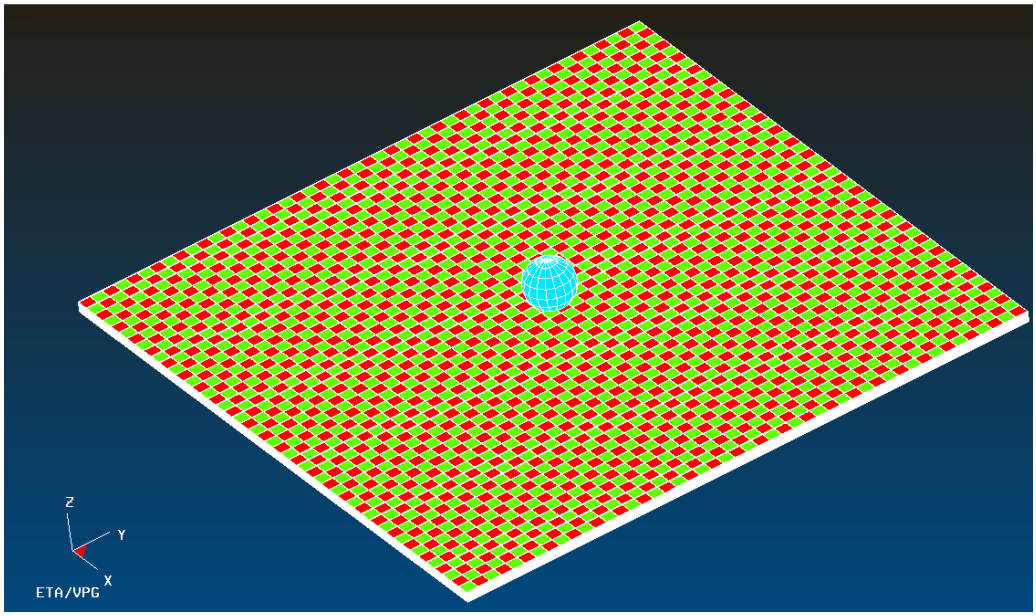

Figure 2.7. Mosaic model in VPG 3.1.1

As shown in the Figure 2.8, the impactor is modeled in VPG 3.1 using a solid sphere with 4-node quad elements. The impactor is modeled as a rigid body and the rigid properties are assigned to the impactor. The resultant properties of the composite's unit cell are defined based on both fiber and matrix properties.

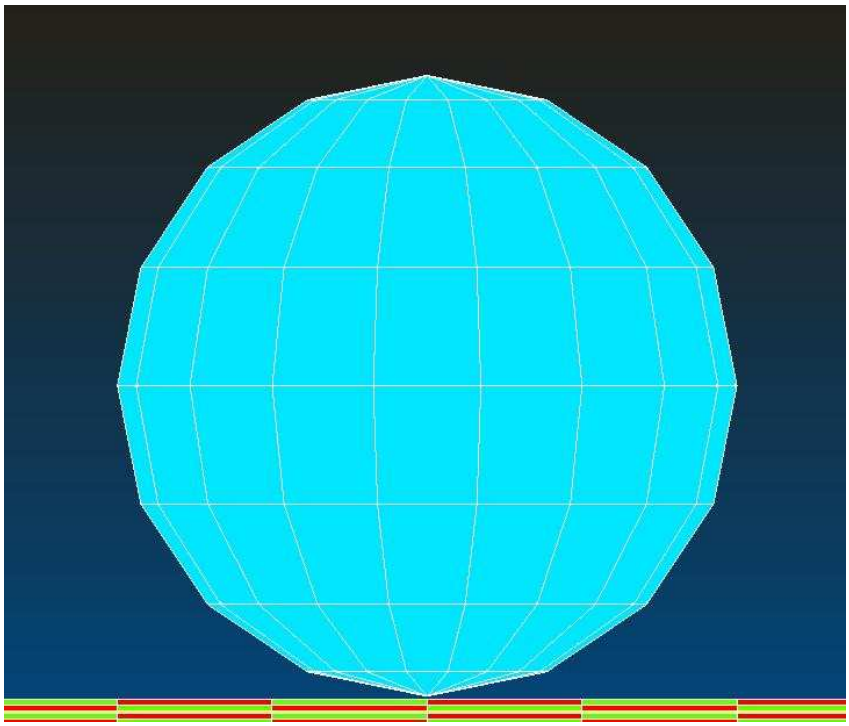

Figure 2.8. Impactor

The COMPOSITE_DAMAGE material card was used to define the composite material. Numerous research studies have been done to derive composite properties. Some of the research works were based on experiments and some of those were based on numerical studies. Chamis [25] provided simplified equations to compute strengths,

fracture toughness and impact properties based on the micro mechanics approach. The following equations were provided by Chamis in his research paper. The longitudinal modulus,

$$E_{l11} = k_f E_{f11} + k_m E_m$$

The transverse modulus,

$$E_{l22} = E_m / (1-\sqrt{k_f}\,(1-E_m/E_{f22})) = E_{l33}$$

The shear modulus,

$$G_{l12} = G_m / (1-\sqrt{k_f}\,(1-G_m/G_{f12})) = G_{l13}$$

$$G_{l23} = G_m / (1- k_f\,(1-G_m/G_{f23}))$$

The Poisson's ratio,

$$\mu_{l12} = k_f \mu_{f12} + k_m \mu_m = \mu_{l13}$$

$$\mu_{l23} = k_f \mu_{f23} + k_m (2 \mu_m - (\mu_{l12}/ E_{l11}) E_{l22}$$

Figure 2.9 shows the direction of fibers in the unit cell. The total number of elements in the model was 67143. The total computation time for each simulation was 11 clock hours. Table 2.1 shows the properties of the impactor which is a steel ball. The density and size of the ball is same as the impactor of actual test.

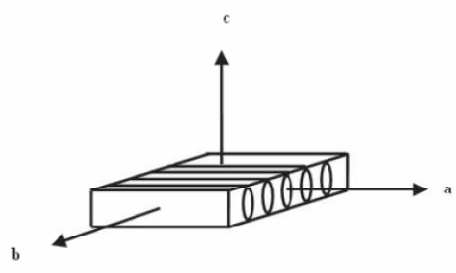

Figure 2.9. Fiber direction in unit cell

Table 2.1 Impactor (steel ball) properties

Density ($lbs^2/in/in^3$)	F (MSI)	Pr
.4713	30	.3000

2.6. Concept of Impact Damage and Modeling

Composites are orthotropic materials. The shape, size, orientation and distribution of the reinforcement and various other features such as matrix, grain size are some of the key parameters which significantly affect the properties of composites. Impact damage in composites is characterized by the impact energy required for the initiation of damage.

The upper bound fails when first reinforcing fiber breaks. When the composite fails gradually between lower and upper bounds, it is called as progressive damage. During progressive damage the load bearing capacity of composite increases. Table 2.2 shows composites constituent's properties and Table 2.3 shows unit cell properties.

Table 2.2. Constituent's elastic properties

PROPERTY	VALUE
Fiber volume fraction K_f	0.50
Matrix volume fraction K_m	0.50
Elastic modulus for matrix E_m(MSI)	0.50
Shear modulus for E-glass G_m (MSI)	0.1851
Elastic modulus for E-glass in longitudinal direction E_{faa} (MSI)	10.60
Elastic modulus For E-glass in transverse direction E_{fbb} (MSI)	10.60
Shear Modulus For E-glass G_{fab} (MSI)	4.37

Table 2.3. E-glass- epoxy unit cell properties

Fiber Orientation	Warf (90 Degree)	Weft (90 Degree)
Density($lbs^2/in/in^3$)	1.58E-04	1.58E-04
E_a(MSI)	5.55	1.532
E_b(MSI)	1.532	5.55
E_c(MSI)	1.532	1.532
G_{ab}(MSI)	.574	.574
G_{bc}(MSI)	.355	.574
G_{ca}(MSI)	.574	.355
Pr_{ba}	.0787	.2850
Pr_{ca}	.0787	.4206
Pr_{cb}	.4206	.0787

gradually, when it reaches its failure stage the load bearing capacity fails drastically. In the present study MAT_COMPSOITE_DAMAGE material card was used to define the material model.

MAT_COMPSOITE_DAMAGE defines a material with five material parameters. This material These are:

S_1, longitudinal tensile strength

S_2, transverse tensile strength

S_{12}, shear strength

C_2, transverse compressive strength

α, nonlinear shear stress parameter

S_1, S_2, S_{12} and C_2 are obtained from material measurement. A is defined by material shear stress-strain measurements. In its simplest form the model represents the orthotropic material failure without considering the interlaminar delamination. The model does have a provision to incorporate laminated shell theory to invoke the transverse shear deformation.

In plane stress, the strain is given in the terms of stress as

$$\varepsilon_1 = \frac{1}{E_1}(\sigma_1 - \upsilon_1\sigma_2)$$

$$\varepsilon_2 = \frac{1}{E_2}(\sigma_2 - \upsilon_2\sigma_1)$$

$$2\varepsilon_{12} = \frac{1}{G_{12}}\tau_{12} + \alpha\tau_{12}^3$$

Where ε, σ, υ, τ are strain, principal stress, Poisson's ratio, shear stress and subscripts denote the principal directions. The third equation defines the nonlinear shear stress parameter α. The fiber matrix shearing term augments each damage mode,

$$\bar{\tau} = \frac{\frac{\tau_{12}^2}{2G_{12}} + \frac{3}{4}\alpha\tau_{12}^4}{\frac{S_{12}^2}{2G_{12}} + \frac{3}{4}\alpha S_{12}^4}$$

Here, $\bar{\tau}$ is the ratio of shear stress to shear strength. Due to the failure stress, matrix of the composite cracks. The matrix cracking criteria can be determined from,

$$F_{matrix} = \left(\frac{\alpha 2}{S2}\right)^2 + \bar{\tau}$$

where failure is assumed whenever $F_{matrix}>1$. Whenever failure occurs (i.e $F_{matrix}>1$), the material constants E_2,G_{12}, υ_1 and υ_2 are set to zero.The compression failure criteria is given as,

$$F_{comp} = \left(\frac{\sigma_2}{2S_{12}}\right)^2 + \left[\left(\frac{C_2}{2S_{12}}\right)^2 - 1\right]\frac{\sigma_2}{C_2} + \bar{\tau}$$

Here failure occurs whenever Fcomp>1. Whenever failure occurs (i.e $F_{comp}>1$), the material constants E_2,G_{12}, υ_1 and υ_2 are set to zero. The final failure mode occurs due to fiber breakage. Failure occurs whenever $F_{fiber}>1$. Whenever failure occurs (i.e $F_{fiber}>1$),

$$F_{\text{fiber}} = \left(\frac{\sigma_1}{S_1}\right)^2 + \overline{\tau}$$

the material constants E_2,G_{12}, υ_1 and υ_2 are set to zero.

The electrospun nanofiber was modeled using 8 nodes solid element. Isotropic Elastic-Plastic with Failure material model was used to define the material properties of electrospun nanofibers. Failure is assumed to occur if , $\varepsilon^p_{eff} > \varepsilon^p_{max}$. Here, ε^p_{eff} is effective plastic strain and ε^p_{max} is failure plastic strain. Table 2.4 shows the properties of electrospun nanofibers.

Table 2.4 Electrospun nanofiber properties

Shear modulus (PSI)	1258000
Failure stress (PSI)	51000
Bulk modulus (PSI)	1910000
Failure strain	0.14

The impact damage is primarily due to tensile stresses; the effect of compressive stresses accounting for crushing failure is neglected in this modeling. Shear stress failure in thin laminates is minimal; it is neglected in modeling damage. Table 2.5 shows the strengths of E glass-epoxy unit cell. It shows the fiber strength and matrix strength.

Table 2.5 E glass –epoxy unit cell strengths

Fiber Orientation	Warf (0 Degree)	Weft (90 Degree)
XT(MSI)	0.157	2E-02
YT(MSI)	2E-02	0.157

2.7. Post Processing Using LS-PREPOST

LS-PrePost is an advanced pre- and post-processor and model editor from Livermore Software Technology Corporation. It prepares input data and processes the results from LS-DYNA analyses. PrePost's major post-processing capabilities include states result animation, fringe component plotting, and XY history plotting. The user interface is easy to use. All data and menus are designed in a logical way to reduce number of mouse clicks and operations. LS-PrePost can be used on all Unix/Linux workstations and MS Windows computers utilizing the OpenGL graphics standard to achieve fast rendering. LS-PrePost is mostly capable of importing, editing and exporting LS-DYNA keyword files for generating LS-DYNA input files. After solving the model using LS-DYNA solver, LS-PrePost can be used to analyze the results. Any deformation, stress or strain of any individual element or global system can be obtained graphically. The deformation and stress generation of individual elements can be tracked in LS-PrePost. It has also the capability of exchanging data with MS Excel. Figure 2.10 shows a window of LS-PrePost. It shows the stress contour and plot of resultant force LS-PrePost also shows the change of different properties like different stress, and strain, reaction forces with time. It also shows all the buttons which are used to obtain state of the object at different time.

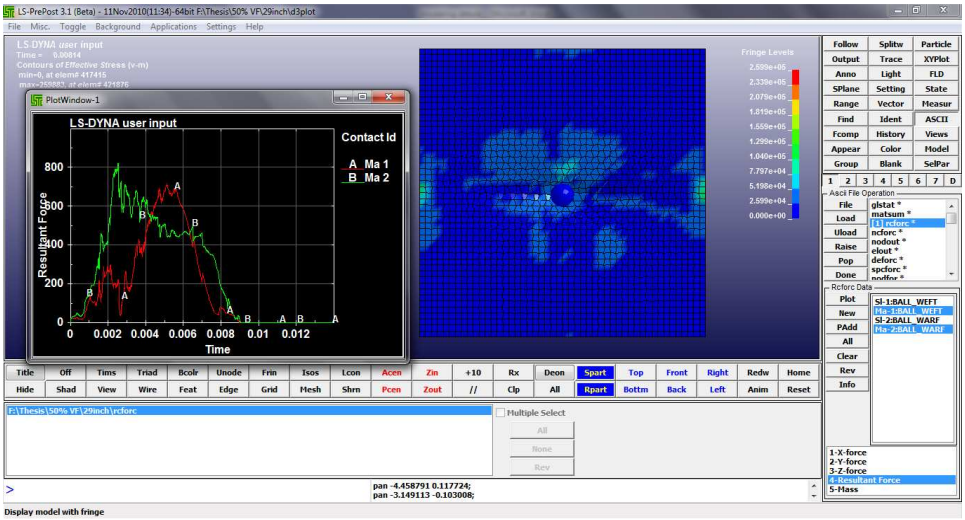

Figure 2.10. Stress contours in LS-PREPOST postprocessor

CHAPTER 3

ANALYSIS OF RESULTS AND DISCUSSION

3.1 Impact Force Response

3.1.1 Impact Response for Each Drop Height

In the following section the experimental impact force versus time results are compared with LSDYNA simulation results. The results are plotted as Impact force (lbf) versus time (ms) for ten (10) ply E-glass composites with and without electrospun nanofibers.

Figures 3.1 through 3.14 show impact force versus time plots for each drop height which corresponds to the respective input energy level. From individual plots it can be seen that simulations results are in good agreement with the experimental results for lower drop height. The simulated maximum impact force is smaller than the experimental value (soft response) at each drop height.

3.1.2 Impact Response for Progressive Damage

The following section shows the experimental and the simulated variation of impact force versus time for five drop heights. It can be seen from the impact force versus time plots, the simulated forces are a bit lower than the experimental forces. At higher energy levels the simulated results shows more failure of laminates. The weakness of the laminates at the higher impact energy levels can be attributed to the fact of using the material models of LSDYNA.

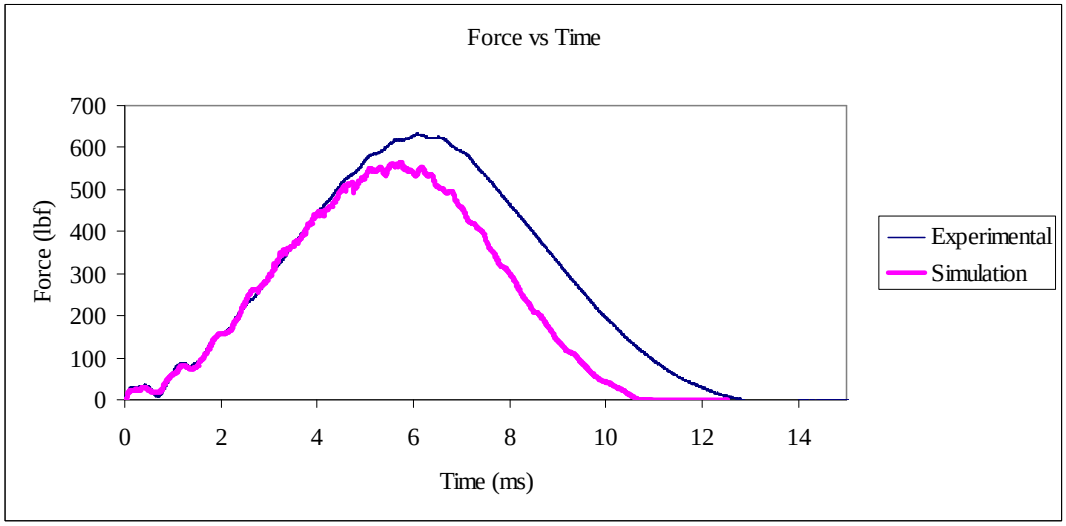

Figure 3.1. Impact force for 10 ply E-glass epoxy 5 inch drop height (without electrospun nanofiber)

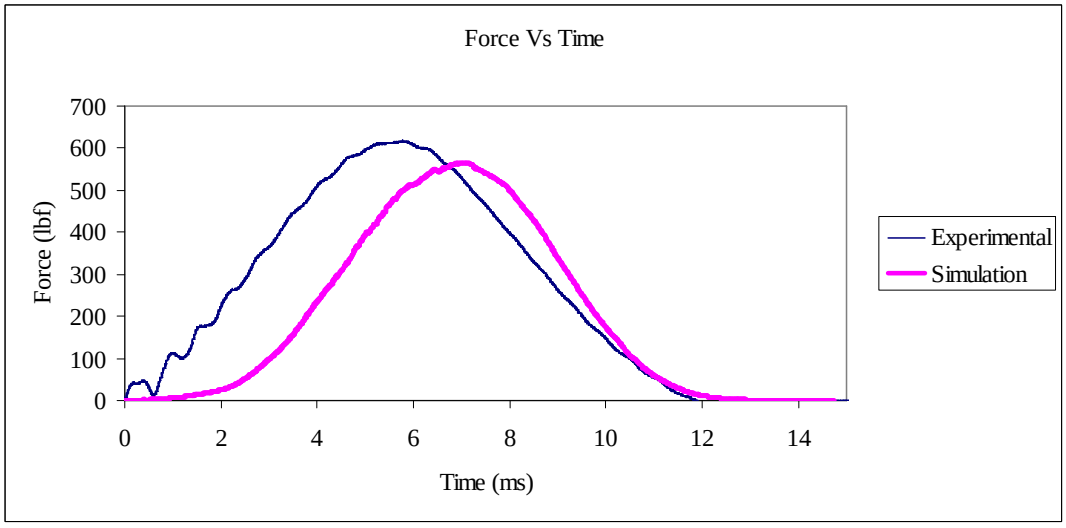

Figure 3.2. Impact force for 10 ply E-glass epoxy 5 inch drop height (with electrospun nanofiber)

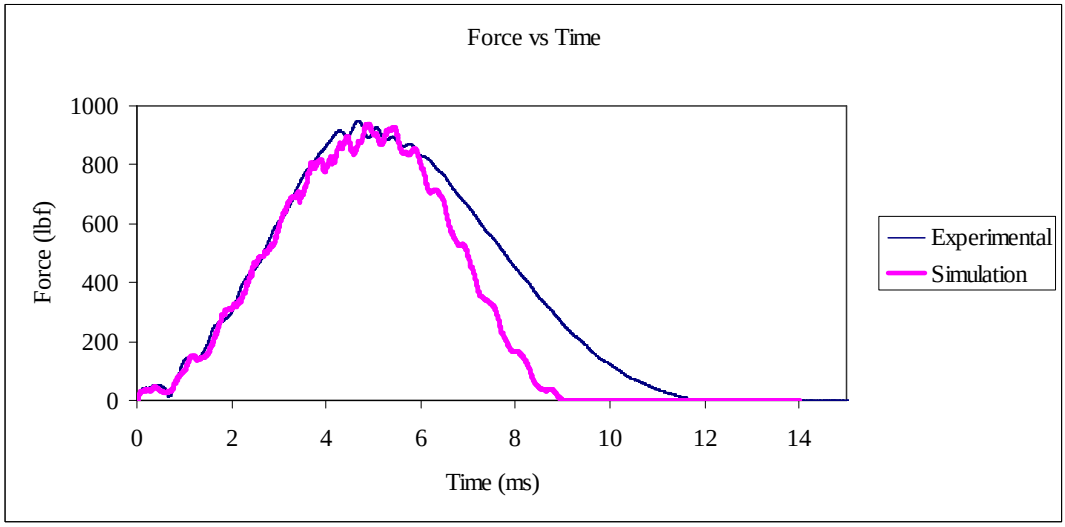

Figure 3.3. Impact force for 10 ply E-glass epoxy 11 inch drop height (without electrospun nanofiber)

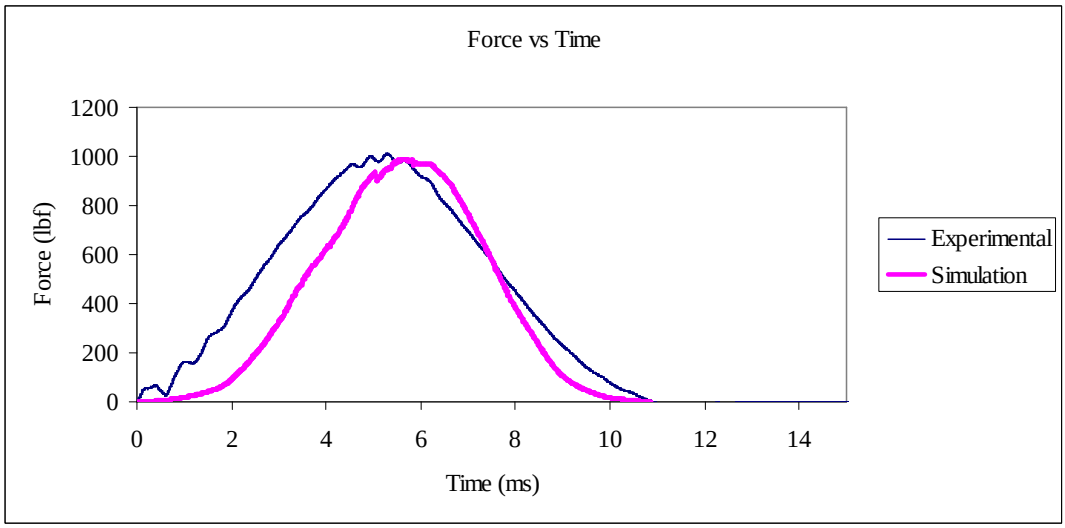

Figure 3.4. Impact force for 10 ply E-glass epoxy 11 inch drop height (with electrospun nanofiber)

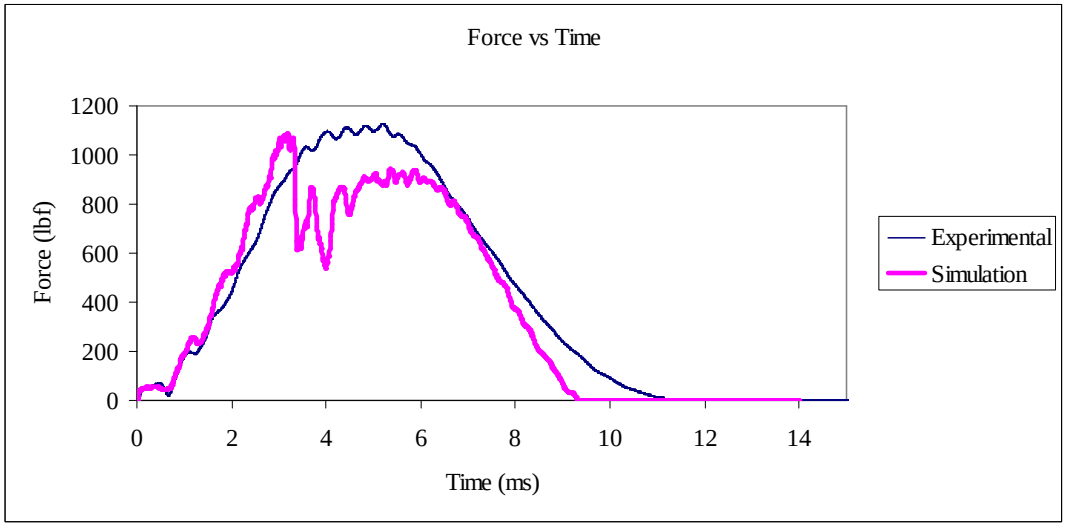

Figure 3.5. Impact force for 10 ply E-glass epoxy 17 inch drop height (without electrospun nanofiber)

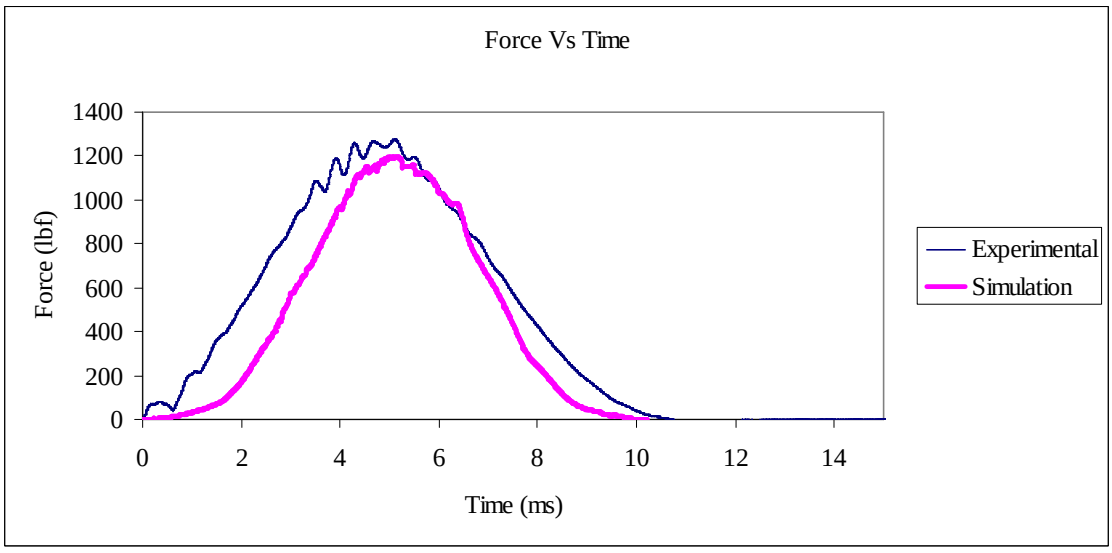

Figure 3.6. Impact force for 10 ply E-glass epoxy 17 inch drop height (with electrospun nanofibers)

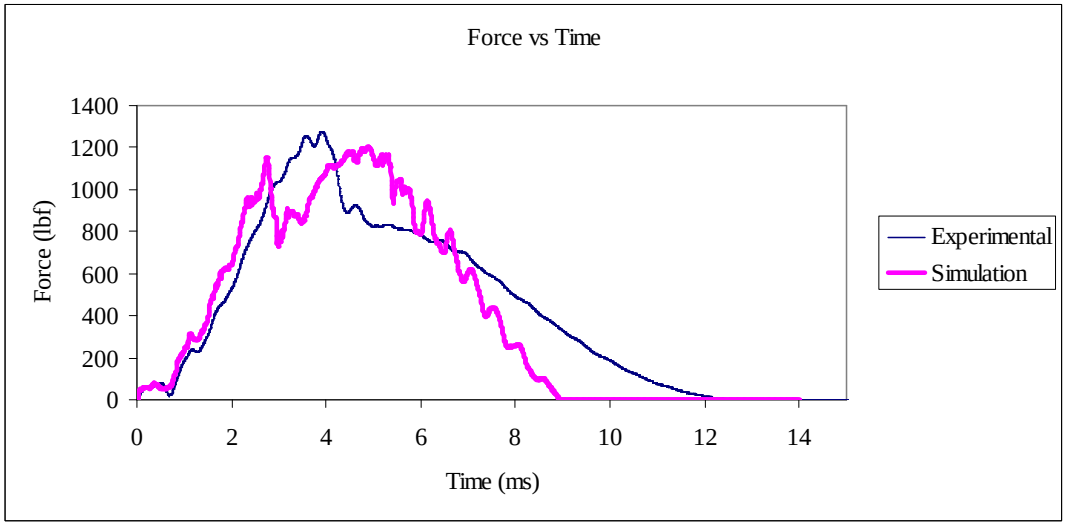

Figure 3.7. Impact force for 10 ply E-glass epoxy 23 inch drop height (without electrospun nanofiber)

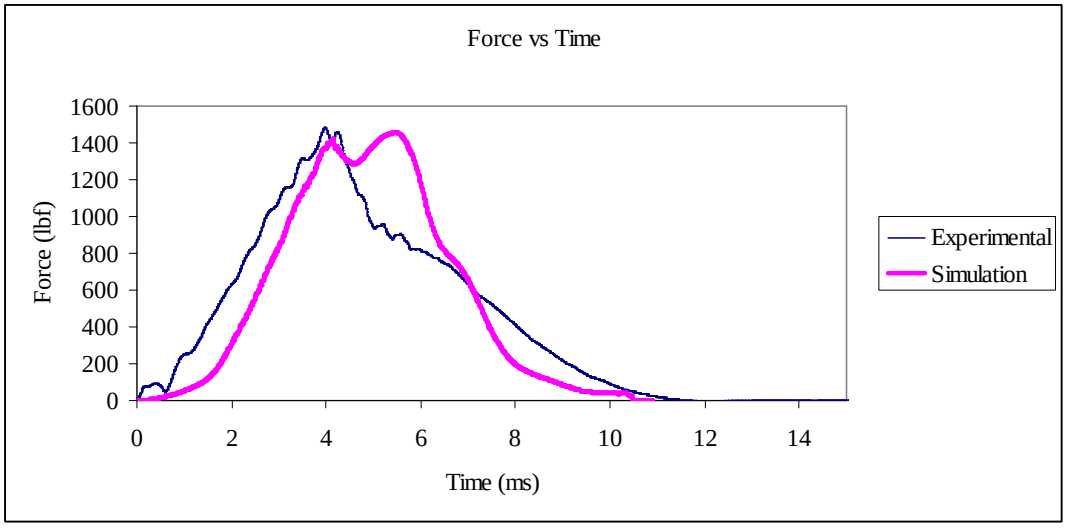

Figure 3.8. Impact force for 10 Ply E-glass epoxy 23 inch drop height (with electrospun nanofiber)

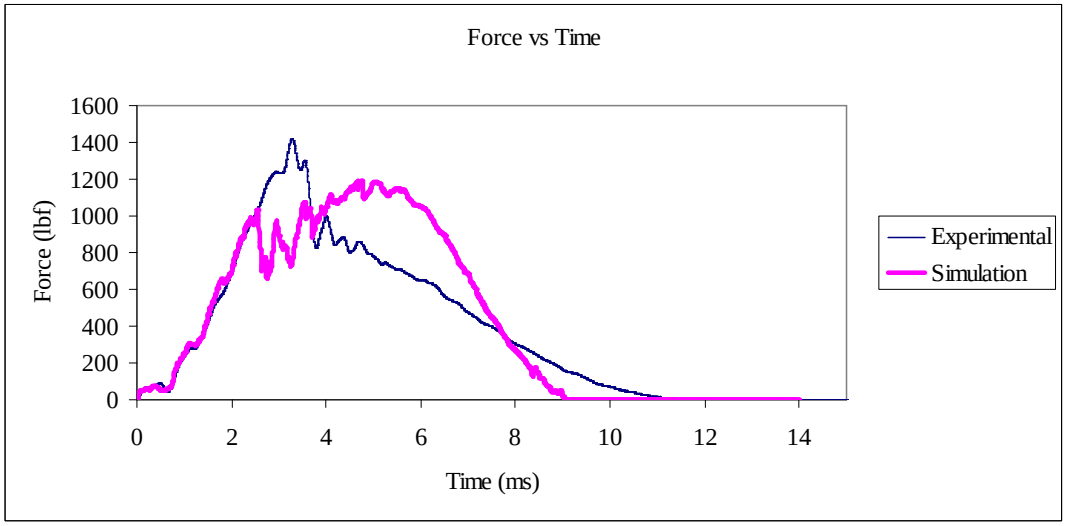

Figure 3.9. Impact force for 10 ply E-glass epoxy 29 inch drop height (without electrospun nanofiber)

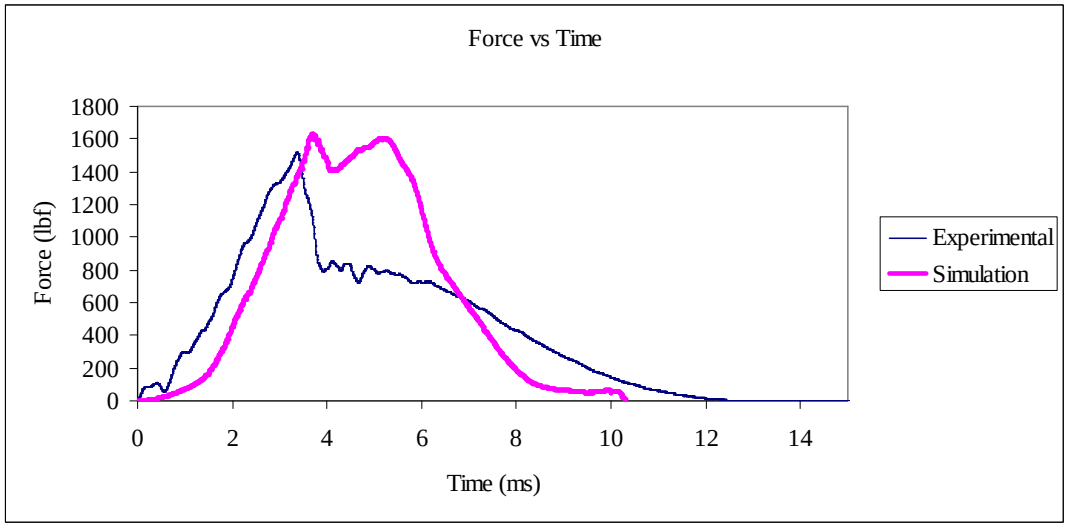

Figure 3.10. Impact force for 10 ply E-glass epoxy 29 inch drop height (with electrospun nanofiber)

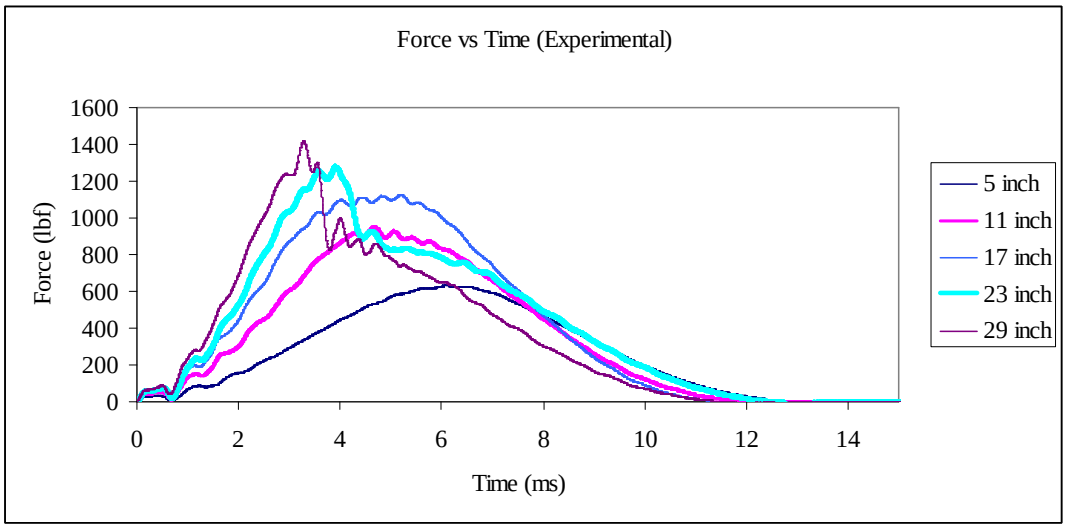

Figure 3.11. Experimental impact force vs. time plot for progressive damage E-glass epoxy laminates (without electrospun nanofiber)

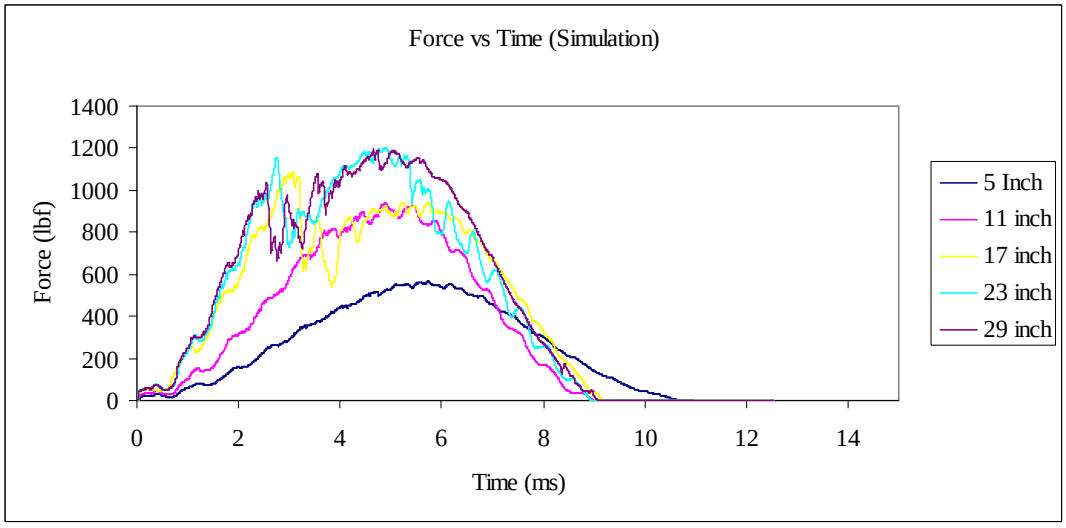

Figure 3.12. Simulated impact force vs. time plot for progressive damage E-glass epoxy laminates (without electrospun nanofiber)

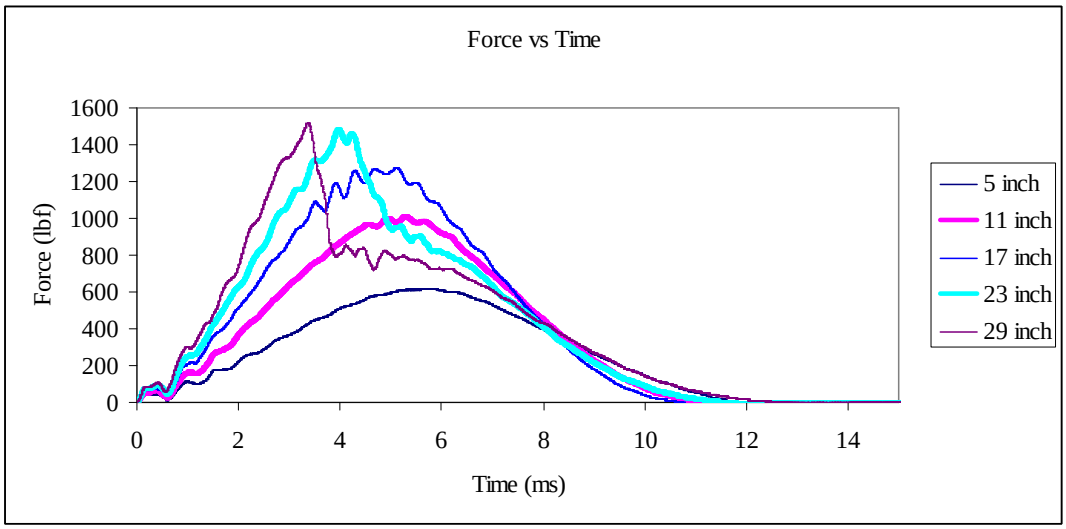

Figure 3.13. Experimental impact force vs. time plot for progressive damage E-glass epoxy laminates (with electrospun nanofiber)

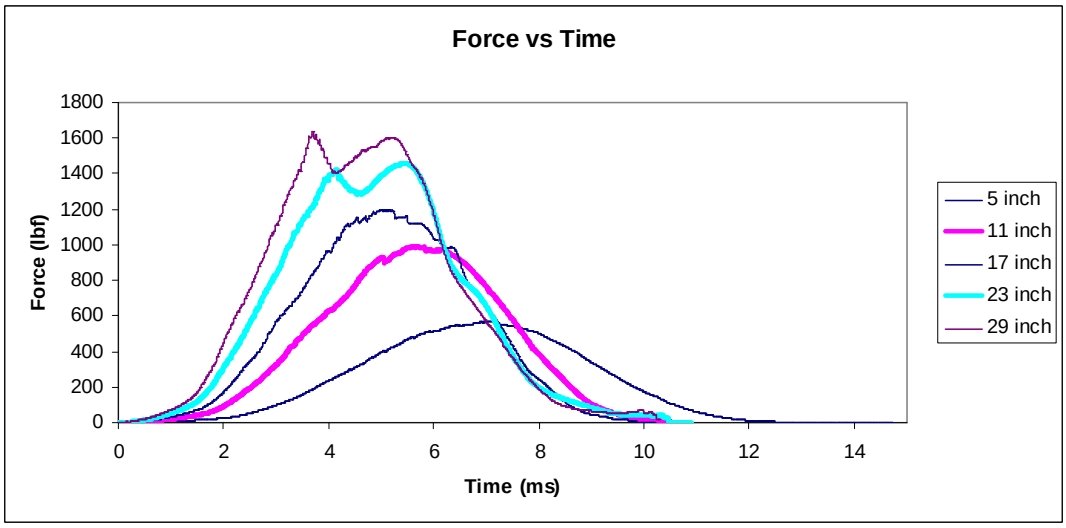

Figure 3.14. Simulated impact force vs. time plot for progressive damage E-glass epoxy laminates (with electrospun nanofiber)

The material model used for this simulation is based on the maximum stress failure criteria, that is, when the stress reaches to maximum value, the element fails and that failed element cannot carry any additional impact force. This may result in to a weaker laminate than the actual experimental conditions, in real case that failed element still may have some capacity left to carry an additional impact force. This material model assumes failure occurs due to in plane stress in unidirectional lamina. In this 2D failure model, the failure modes due to out of plane shear or normal stresses are neglected. So this model is unable to capture transverse impact failures for which all six stress components are known to contribute to the development of damage.

3.2 Analysis of Results

At lower energy levels like the 5 inch and 11 inch drop height, the impact responses are almost same. As the energy level goes higher, the area under Impact Force vs time increases when electrospun nanofibers are used. The impact duration also increases when electrospun nanofibers are used. Impact duration increases due to damage of electrospun nanofibers. As the impactor hit the composite surface, electrospun nanofibers in between layers absorb energy and fail. Nanofiber layers dissipate the energy and increases the impact duration.

In the present model the mesh size of the composite is larger than the mesh size of the impactor. So when the initial contact occurs, the impact force is not experienced immediately by the composite panel. Once the impactor comes in contact with a node of the composite panel, it experiences the impact force. Due to this reason the simulated

impact force becomes different than the experimental impact forces. Figures 3.15 to 3.24 show the effect of electrospun nanofibers on impact responses. The figures compare the experimental results of impact with and without nanofibers. The figures also compare the simulation results of impact with and without nanofibers.

It can be observed that the simulated results do not follow the experimental results at higher energy levels when nanofibers are inserted in between layers of composites. In this study, volume fraction of nanofibers was assumed to be 50% .The strength, modulus of elasticity and poisson's ratio of the composite depends of the volume fraction of the composites. In this case the exact volume fraction was not available. When the actual experiments were performed, the nanofibers may have failed due to failure strain. So during the experiments whenever there was a failure, it was reflected in the impact load vs time plot. In this study, it was assumed that nanofibers fail only due to fiber failures, but nano-fibers can also fail due to strain. The exact failure strain of nanofibers was not available. As a result the simulation results do not follow exactly the experimental results.

Figure 3.25 and Figure 3.26 show the maximum impact load variation of the composite with and without nanofibers at different drop heights. Basically these figures compare the maximum impact load experienced by the plate during experiments and simulations. It is observed that composite with nanofibers experience a bit higher force at higher energy level compared to composites at lower energy levels. The experimental results of maximum impact load are higher than simulation results. These two results exactly did not match because of assumptions of failure criteria in simulations.

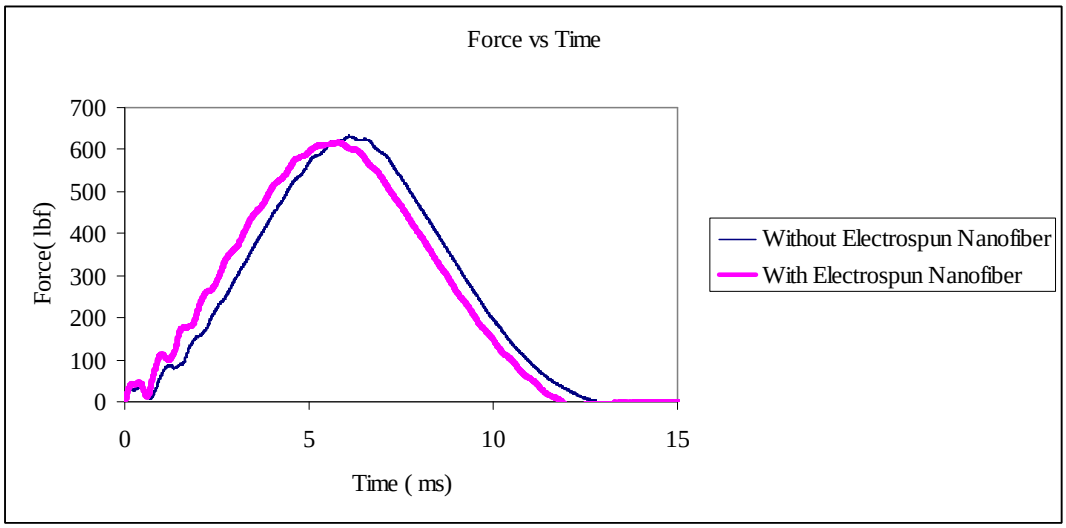

Figure 3.15. Effect of electrospun nanofibers on impact response (experimental results at 5 inch drop height)

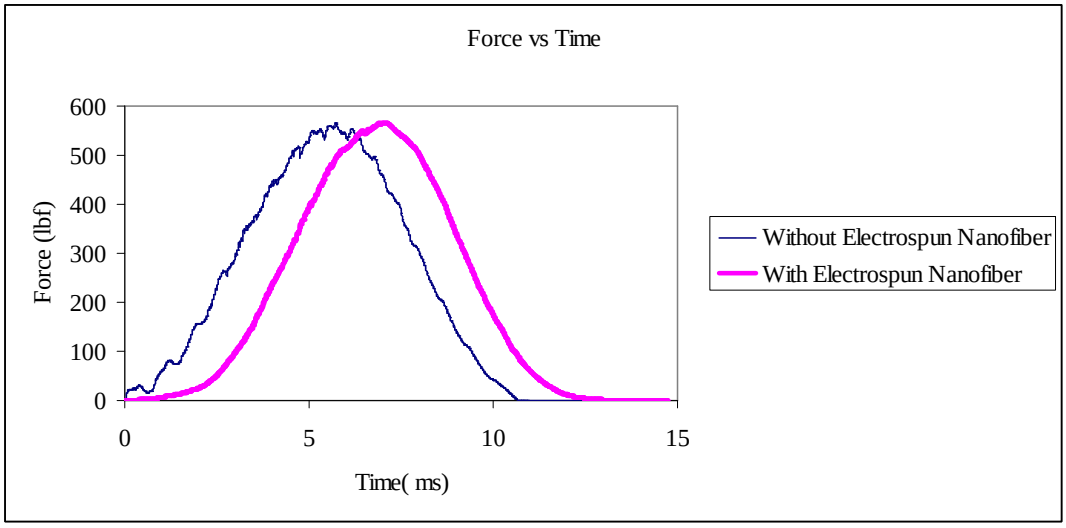

Figure 3.16. Effect of electrospun nanofibers on impact response (simulation results at 5 inch drop height)

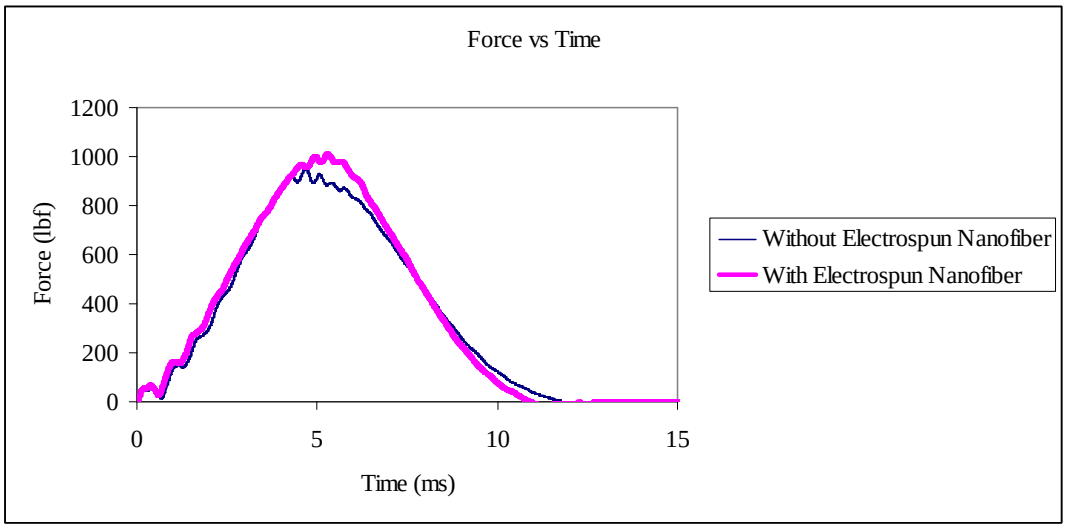

Figure 3.17. Effect of electrospun nanofibers on impact response (experimental results at 11 inch drop height)

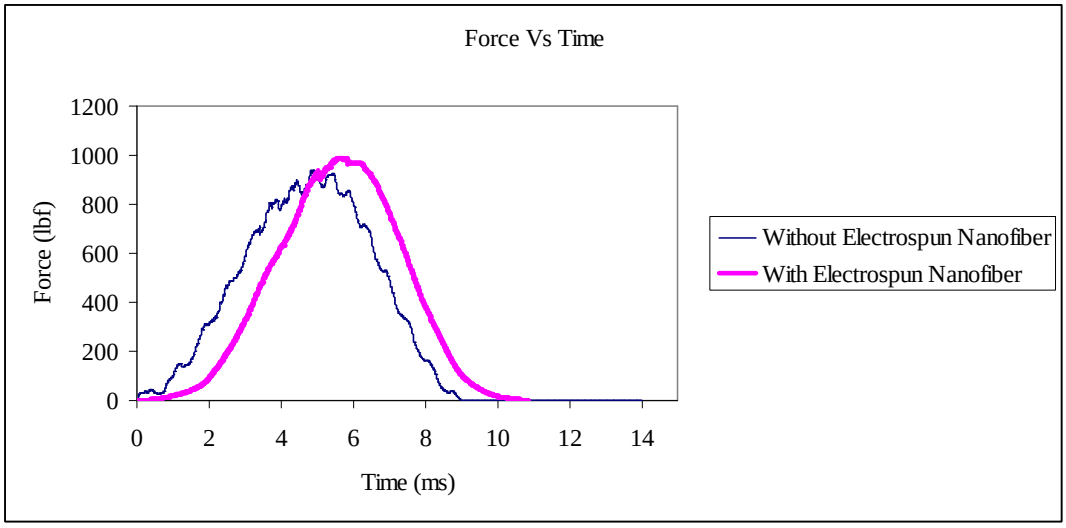

Figure 3.18. Effect of electrospun nanofiber on impact response (simulation results at 11 inch drop height)

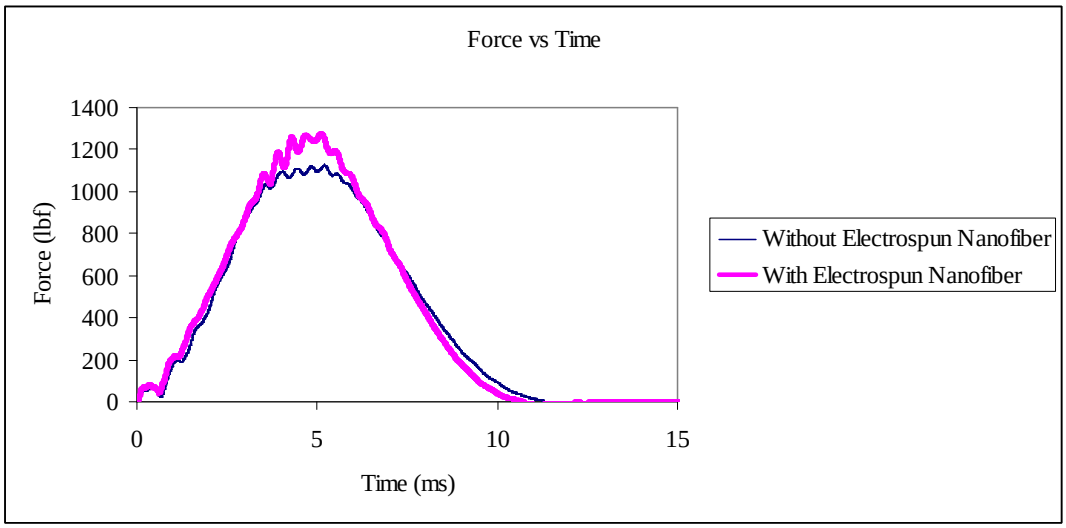

Figure 3.19. Effect of electrospun nanofiber on impact response (experimental results at 17 inch drop height)

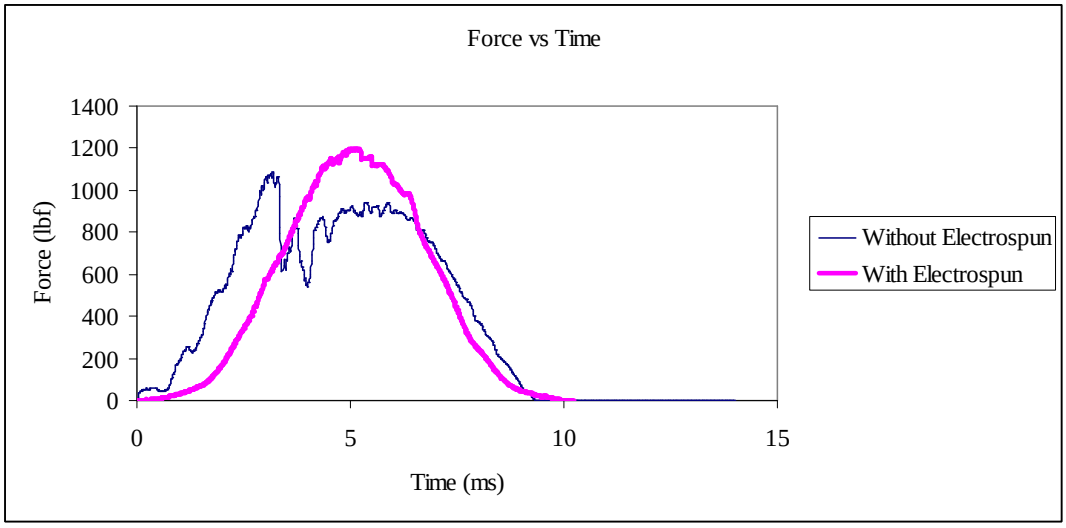

Figure 3.20. Effect of electrospun nanofibers on impact response (simulation results at 17 inch drop height)

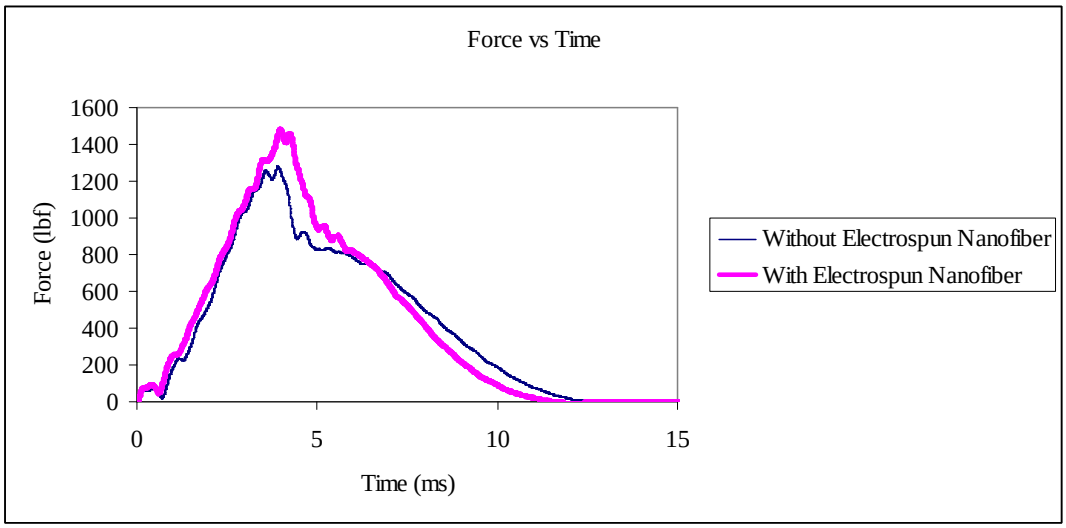

Figure 3.21. Effect of electrospun nanofibers on impact response (experimental results at 23 inch drop height)

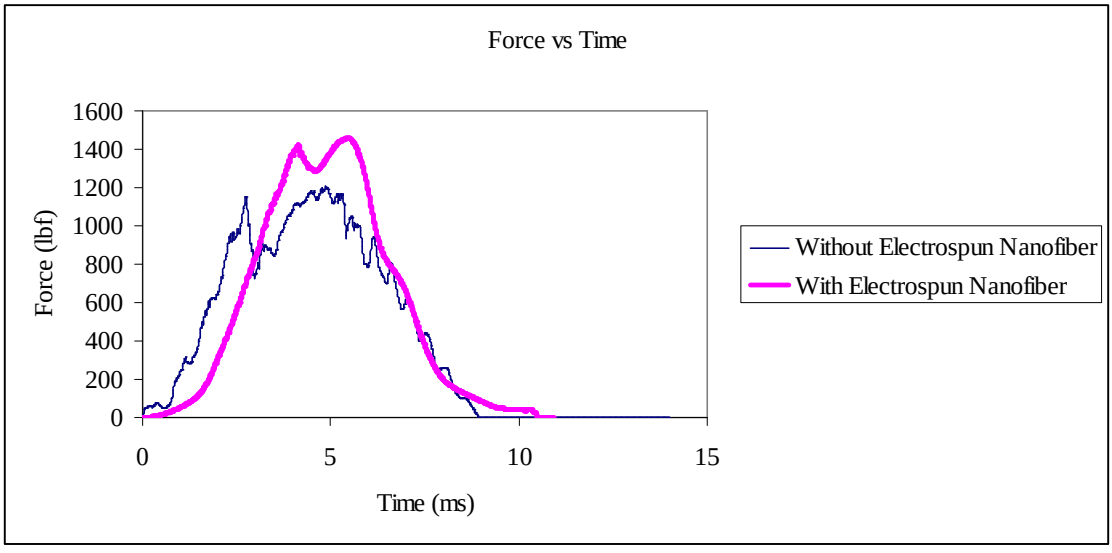

Figure 3.22. Effect of electrospun nanofibers on impact response (simulation results at 23 inch drop height)

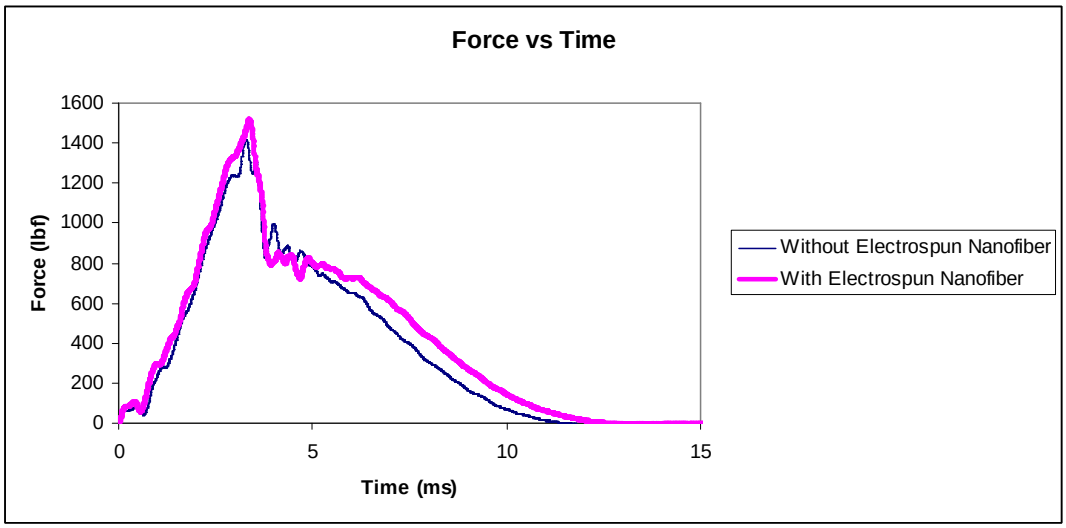

Figure 3.23. Effect of electrospun nanofibers on impact response (experimental results at 29 inch drop height)

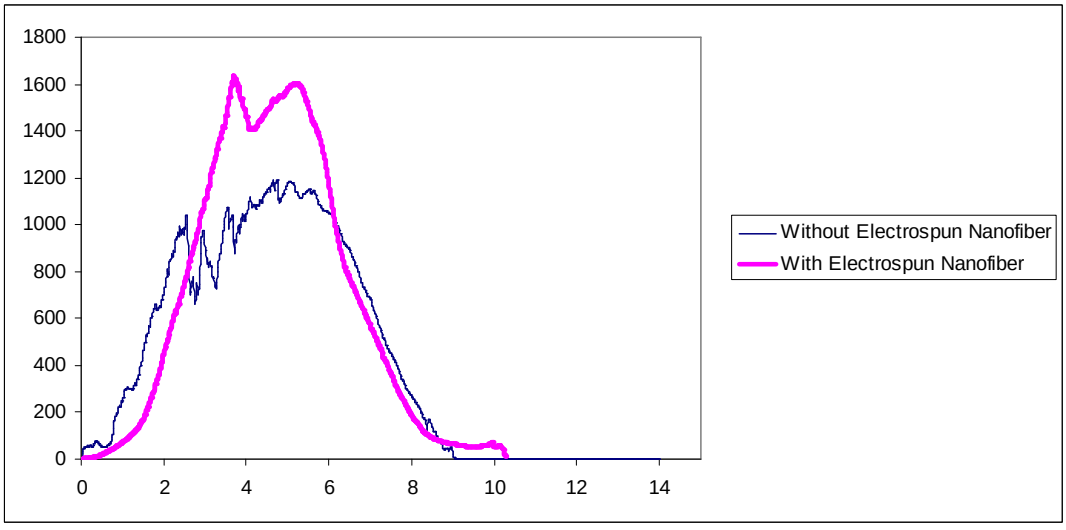

Figure 3.24. Effect of electrospun nanofibers on impact response (simulation Results at 29 inch drop height)

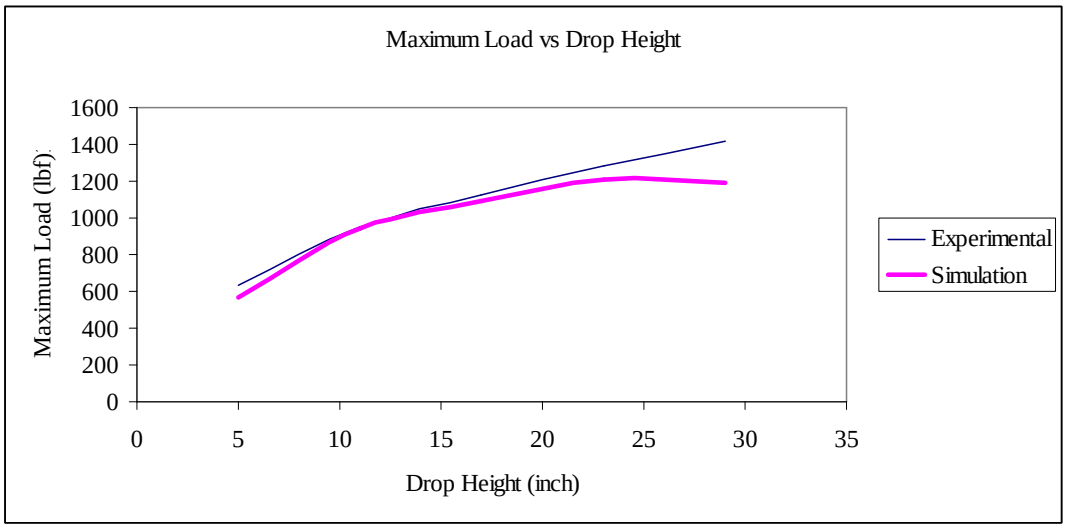

Figure 3.25. Maximum load vs drop height (without electrospun nanofibers)

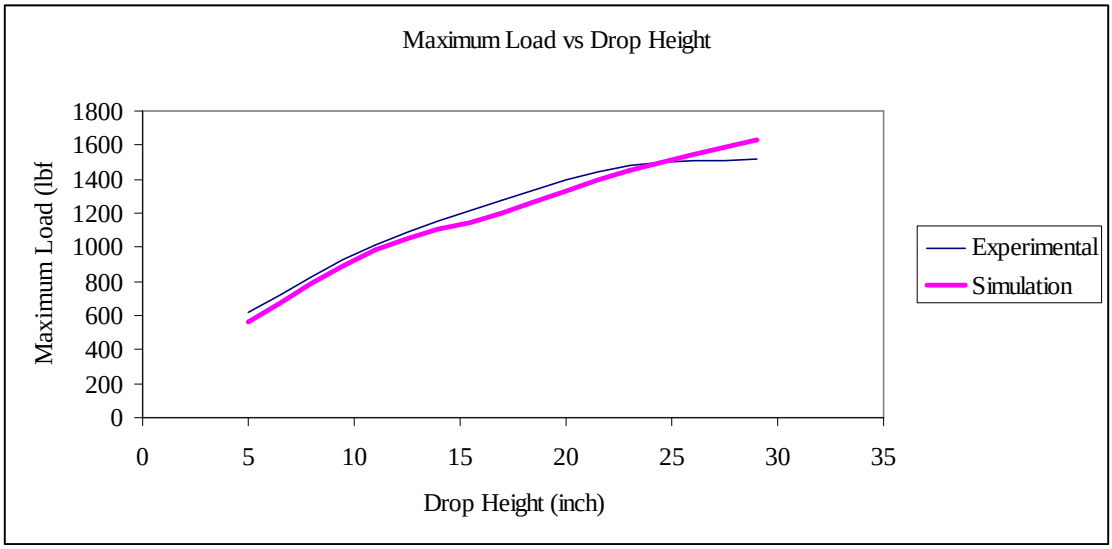

Figure 3.26. Maximum load vs drop Height (with electrospun nanofibers)

Figures 3.27 to 3.36 show the maximum stress contour of composite at different drop heights. It was observed that nanofibers reduce the maximum stress in composites. When nanofibers are inserted in between layers the stress is distributed throughout the composite panel. Without nanofibers the stress is more concentrated in one area. From Figure 3.33 to 3.36 it can be observed that at higher energy input levels the stress is concentrated into just the impact area when nanofibers are not used. When nanofibers are used, the stress is distributed throughout the composite panels and resulting maximum stress is less than that of the composite with nanofibers.

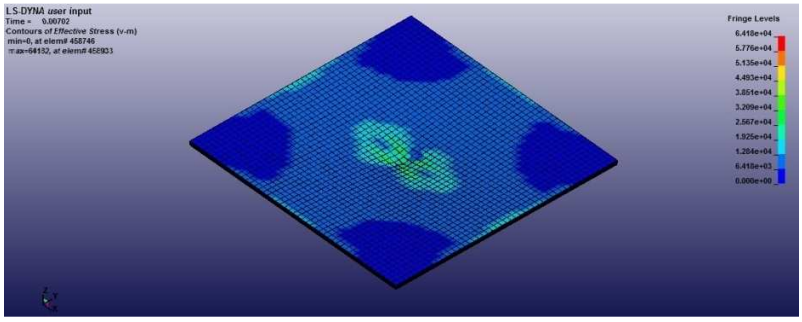

Figure 3.27. Maximum Von-mises stress with nanofibers (5 inch drop height)

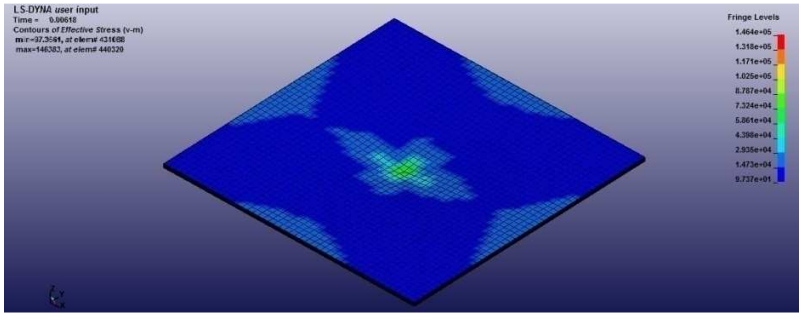

Figure 3.28. Maximum Von-mises stress without nanofibers (5 inch drop height)

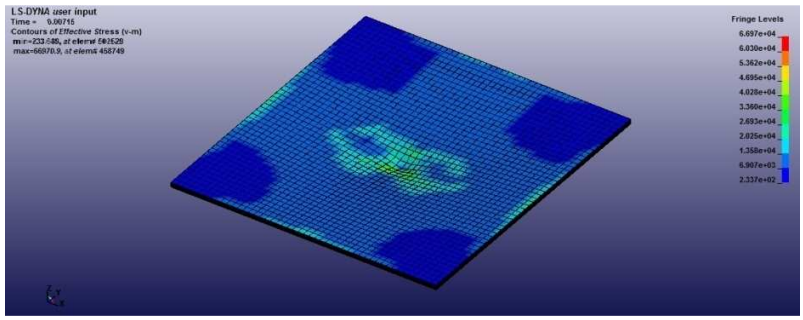

Figure 3.29. Maximum Von-mises stress with nanofibers (11 inch drop height)

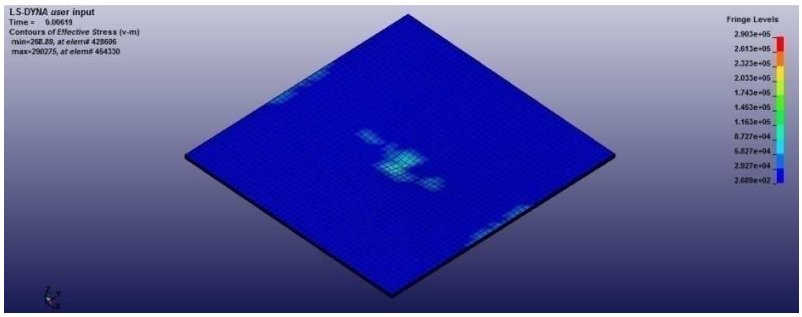

Figure 3.30. Maximum Von-mises stress without nanofibers (11 inch drop height)

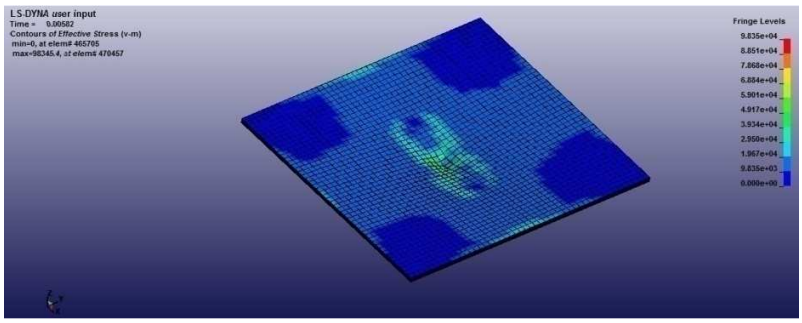

Figure 3.31. Maximum Von-mises stress with nanofibers (17 inch drop height)

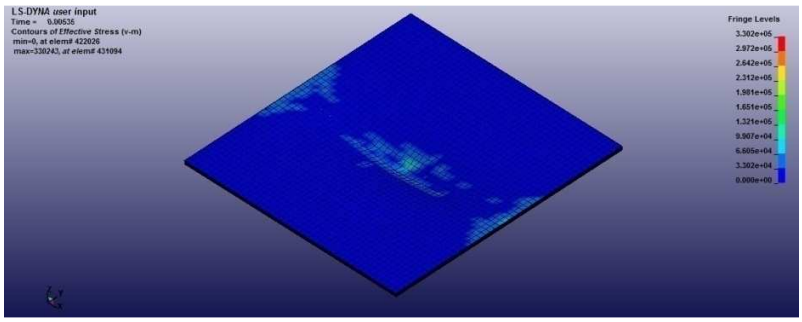

Figure 3.32. Maximum Von-mises stress without nanofibers (17 inch drop height)

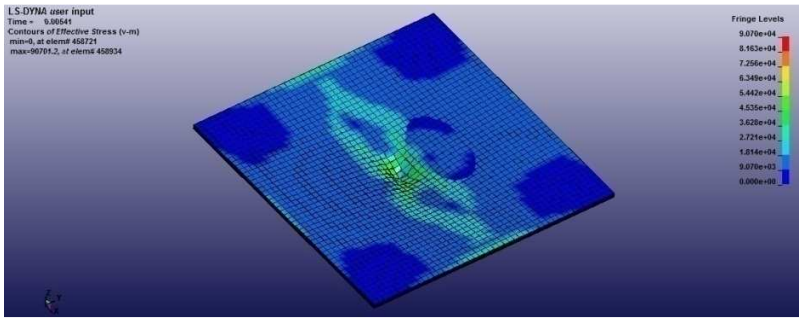

Figure 3.33. Maximum Von-mises stress with nanofibers (23 inch drop height)

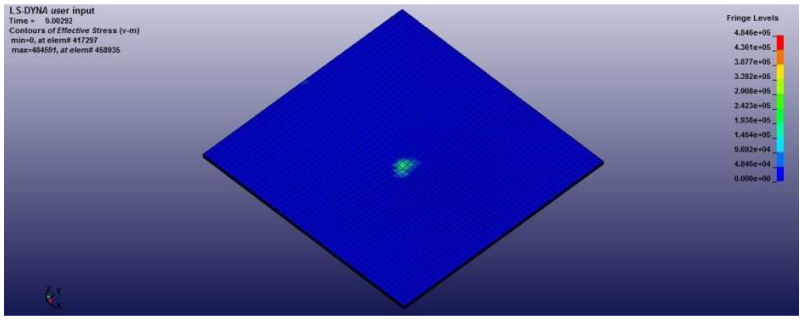

Figure 3.34. Maximum Von-mises stress without nanofibers (23 inch drop height)

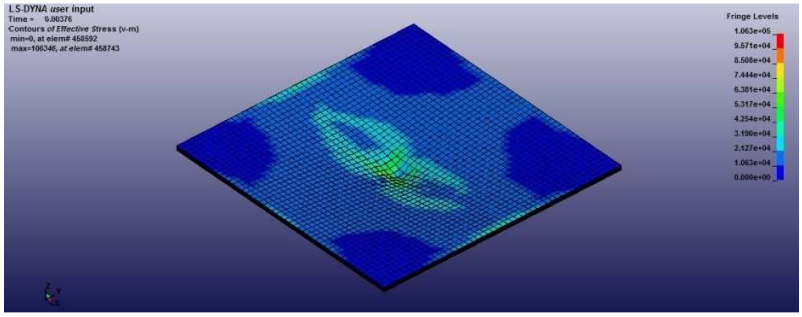

Figure 3.35. Maximum Von-mises stress with nanofibers (29 inch drop height)

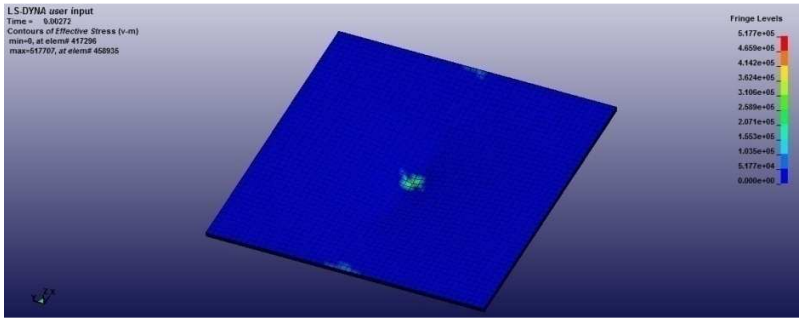

Figure 3.36. Maximum Von-mises stress without nanofibers (29 inch drop height)

CHAPTER 4

CONCLUSION AND FUTURE SCOPE OF RESEARCH

In the present study the progressive impact responses of 10 ply E-glass composite with and without electrospun nanofibers were investigated and validated with experimental data. The composite panel was modeled using the mosaic model and simulated using LSDYNA. It was found that the simulated responses for composites were in good harmony with experimental responses at lower energy levels where lower damage occurs. For higher energy levels, the simulated impact loads are lesser than the experimental impact loads which results in less bending stiffness and weaker laminate. In this study, it was assumed that volume faction of nanofibers is 50%. The actual volume fraction was not available. It was also assumed that nanofibers fails only because of fiber failures. But in real life, nanofiber can fail due to strain. The actual failure strain of nanofibers was not available. So the nanofibers should be tested to determine their failure strain and volume fraction. Further development of material models for progressive material damage is recommended.

Preliminary study shows that inserting electrospun nanofibers increases the impact resistance of composites. Further investigation using an ultrasonic C scan would be helpful in understanding the inter-laminar damage quantitatively and qualitatively. An ultrasonic C scan will help to understand the failure of the composite at different drop heights. If the failure mechanism is understood better through ultrasonic C scan, the failure criteria can be used more effectively in computational modeling. The composite

panel modeling approach can be improved. The mosaic model is an approximate model. Further investigation should be done for modeling exact undulation of fibers.

When the mesh size of the composite is larger than the mesh size of the impactor, the simulated impact force offsets from the experimental impact forces. The mesh size of composite can be decreased in order to get better results.

REFERENCES

[1] Bird strike http://en.wikipedia.org/wiki/Bird_strike

[2] http://en.wikipedia.org/wiki/File:JT8D_Engine_after_Bird_Strike.jpg

[3] http://en.wikipedia.org/wiki/Bird_strike

[4] http://en.wikipedia.org/wiki/File:C-130_and Hawk in nosecone outside.jpg

[5] http://en.wikipedia.org/wiki/File:IAF_UH-60 after birds strike outside.jpg

[6] http://www.wired.com/defenseJ.F. Cooley “Apparatus for Electrically Dispersing Fluids”.

[7] Doucet JP, Weber J. Computer-aided molecular design: theory and applications. London: Academic Press; 1996.

[8] Shendokar, Sachin, “Manufacturing and characterization of advanced delamination resistant composite interleaved with electrospun nanofibers”. PhD thesis, 2010, North Carolina Agricultural and Technical State University, Greensboro, North Carolina, USA.

[9] Rotem, A, Lifshitz, JM. “Longitudinal strength of unidirectional fibrous composite under high rate if loading”.In: proc 26th Annual Tech Conf Soc Plastics Industry Reinforced Plastics, Composites Division, Washington, DC, 1971. Section 10-G

[10] Lifshitz, JM. “Impact strength of angle ply fiber reinforced materials”. J Compos Mater 1976; 10:92–101.

[11] Sierakowski, RL, Nevil, GE, Ross, A, Jones, ER. “Dynamic compressive strength and failure of steel reinforced epoxy composites”. J Compos Mater 1971;5:362–77.

[12] Sankar, BV. “Scaling of low-velocity impact for symmetric composite laminates”. J Reinf Plast Compos 1992;11:297–305.

[13] Wang, X., Hu, B., Feng,Y., Liang, F., Mo, J., Xiong, J., Qiu, Y., “Low Velocity Impact Properties of 3D Woven Basalt/ Aramid Hybrid Composites”. ELSEVIER CSTE 3751, S0266-3538 (07) 00260-6

[14] Sarah E. Mouring, Luke Louca, William Levis, “Structural Response of Impact-

Damaged Composite Panels".

[15] Krishnan, Vijay. "Performance Evaluation and Modeling of Woven Roving Glass, Stitch Bonded Glass and Stitched Bonded Carbon Composites subjected to Low Velocity Impact Loads". Master's Thesis 2004, North Carolina A&T State University, Greensboro, North Carolina, USA.

[16] Zukas, Jonas A. "Introduction to penetration mechanics." High Velocity Impact Dynamics. Ed. Jonas A, Zukas,1990

[17] Lee, S. W. R., Sun C.T. "Dynamic penetration of graphite/epoxy laminates by a blunt-ended projectile". Composite Science and Technology, Vol. 49, 1993, pp. 399-421.

[18] Al, Mines, "High velocity perforation behavior of polymer composite laminates", International Journal Impact Engineering Vol. 22, 1999, pp. 561-588.

[19] Zheng, Xiahua, Goldberg, Robert K, Binienda, Wieslaw K., Roberts, Gary D., "LSDYNA implementation of Polymer Matrix Composite Model under high strain rate impact". NASA/ TM-2003-212583

[20] Thatte , Bhushan, "Experimental and analytical investigation of low velocity impact response of hybrid composite using LSDYNA". Master's Thesis 2009, North Carolina A&T State University, Greensboro, North Carolina, USA.

[21] Johnson, Alastair F., Nathalie, Pentecote, "Modelling Impact damage in Double-Walled Composite Structures", VIII International Conference on Computational Plasticity COMPLAS VIII E Onate and D.R. J. Owen (Eds) © CIMNE, Barcelona,2005

[22] Ipson, T.W and R.F Recht. "Ballistic-penetration resistance and its measurement." Vol. 15. Pp 247-256, 1975

[23] Livermore Software technology Corporation, LS- DYNA Theoretical Manual, Livermore, California.

[24] Shirolikar, Alok, "Progressive Damage Analysis of Impact on Woven Roven Composites using LS- DYNA®", (2006) Master's Thesis, North Carolina A&T State University, Greensboro NC 27411, USA

[25] Chamis, Christos C. (1986), "Simplified Composite Micromechanics for Predicting Microstresses". 41st Annual Conference, Reinforced Composites Institute, The Society of the Plastic Industry Inc. January 27-31, 1986.

APPENDIX

SAMPLE DYNA INPUT FILE

```
$---+----1----+----2----+----3----+----4----+----5----+----6----+----7-
---+----8
$ LS-DYNA(971) DECK WAS WRITTEN BY: eta/VPG VERSION 3.4
$
$ ENGINEER:
$  PROJECT:
$    UNITS: IN, LB*S*S/IN, SEC, LB
$     DATE:  Dec 28, 2010 at 17:52:47
$
$    NOTES:
$
$---+----1----+----2----+----3----+----4----+----5----+----6----+----7-
---+----8
$ VIEWING INFORMATION
$ -.602716E+000.643544E+01-.205045E+010.186535E+01
$ 0.996665E+00-.681514E-010.448911E-01
$ -.358225E-010.128944E+000.991005E+00
$ -.733248E-01-.989307E+000.126075E+00
$---+----1----+----2----+----3----+----4----+----5----+----6----+----7-
---+----8
*KEYWORD
$---+----1----+----2----+----3----+----4----+----5----+----6----+----7-
---+----8
*TITLE

$---+----1----+----2----+----3----+----4----+----5----+----6----+----7-
---+----8
*CONTROL_CPU
$   cputim     iglst
       0.0         0
*CONTROL_OUTPUT
$    npopt    neecho    nrefup    iaccop     opifs    ipnint    ikedit
iflush
         0         0         0         0       0.0         0       100
5000
$    iprtf    ierode     tet10    msgmax    ipcurv
         0         0         2        50         0
*CONTROL_TERMINATION
$   endtim    endcyc     dtmin    endeng    endmas
   0.03000         0       0.0       0.0       0.0
*CONTROL_TIMESTEP
$   dtinit    tssfac      isdo    tslimt     dt2ms      lctm     erode
ms1st
 .10000E-5   0.90000         0       0.0       0.0         0         1
0
$   dt2msf   dt2mslc     imscl
       0.0         0         0
$---+----1----+----2----+----3----+----4----+----5----+----6----+----7-
---+----8
*DATABASE_DEFGEO
$       dt    binary      lcur     ioopt
 .10000E-4         1         0         0
*DATABASE_DEFORC
$       dt    binary      lcur     ioopt
 .10000E-4         1         0         0
*DATABASE_ELOUT
```

```
$       dt    binary      lcur     ioopt
 .10000E-4         1         0         0
*DATABASE_GLSTAT
$       dt    binary      lcur     ioopt
 .10000E-4         1         0         0
*DATABASE_MATSUM
$       dt    binary      lcur     ioopt
 .10000E-4         1         0         0
*DATABASE_NCFORC
$       dt    binary      lcur     ioopt
 .10000E-4         1         0         0
*DATABASE_NODFOR
$       dt    binary      lcur     ioopt
 .10000E-4         1         0         0
*DATABASE_NODOUT
$       dt    binary      lcur     ioopt      dthf     binhf
 .10000E-4         1         0         0         1         1
*DATABASE_RCFORC
$       dt    binary      lcur     ioopt
 .10000E-4         1         0         0
*DATABASE_SLEOUT
$       dt    binary      lcur     ioopt
 .10000E-4         1         0         0
*DATABASE_SPCFORC
$       dt    binary      lcur     ioopt
 .10000E-4         1         0         0
$---+----1----+----2----+----3----+----4----+----5----+----6----+----7-
---+----8
*DATABASE_BINARY_D3PLOT
$  dt/cycl      lcdt      beam     npltc
 .10000E-4         0         0         0
$    ioopt
         0
*DATABASE_BINARY_D3THDT
$  dt/cycl      lcdt
 .10000E-4         0
$---+----1----+----2----+----3----+----4----+----5----+----6----+----7-
---+----8
*PART
warf
$      pid     secid       mid     eosid      hgid      grav    adpopt
tmid
         1         4         3         0         0         0         0
0
*PART
weft
         2         4         4         0         0         0         0
0
*PART
ball_element
         5         4         1         0         0         0         0
0
*PART
electrospun
         3         4         5         0         0         0         0
0
$---+----1----+----2----+----3----+----4----+----5----+----6----+----7-
---+----8
*SECTION_SOLID_TITLE
solid
$    secid    elform       aet
```

```
         4         1         0
$---+----1----+----2----+----3----+----4----+----5----+----6----+----7-
---+----8
*MAT_COMPOSITE_DAMAGE_TITLE
mat_1
$      mid        ro        ea        eb        ec      prba      prca
prcb
         3  .1645E-3  5550000.  1532580.  1532580.   0.07870   0.07870
0.42060
$      gab       gbc       gca     kfail      aopt      macf
  574000.0  355000.0  574000.0       0.0     2.000     1.000
$       xp        yp        zp        a1        a2        a3
       0.0       0.0       0.0     1.000       0.0       0.0
$       v1        v2        v3        d1        d2        d3      beta
       0.0       0.0       0.0       0.0     1.000       0.0       0.0
$       sc        xt        yt        yc      alph        sn       syz
szx
 .1290E+6 .1570E+6  20000.00 -.186E+10       0.0 .1000E+16 .1000E+16
.1000E+16
*MAT_COMPOSITE_DAMAGE_TITLE
mat_b
$      mid        ro        ea        eb        ec      prba      prca
prcb
         4  .1645E-3  1532580.  5550000.  1532580.   0.28500   0.42060
0.07870
$      gab       gbc       gca     kfail      aopt      macf
  574000.0  574000.0  355000.0       0.0     2.000     1.000
$       xp        yp        zp        a1        a2        a3
       0.0       0.0       0.0     1.000       0.0       0.0
$       v1        v2        v3        d1        d2        d3      beta
       0.0       0.0       0.0       0.0     1.000       0.0       0.0
$       sc        xt        yt        yc      alph        sn       syz
szx
 .1290E+6  20000.00 .1570E+6 -.186E+10       0.0 .1000E+16 .1000E+16
.1000E+16
*MAT_RIGID_TITLE
BALL MAT
$      mid        ro         e        pr         n    couple         m
alias
         1   0.47133  .3000E+8   0.30000       0.0       0.0       0.0
0.0
$      cmo      con1      con2
       0.0         0         0
$      lco
       0.0
*MAT_ISOTROPIC_ELASTIC_FAILURE_TITLE
nanofiber
$      mid        ro         g      sigy      etan      bulk
         5  .1066E-3  1258000.  51000.00       0.0  1910000.
$      epf       prf       rem      trem
   0.90000       0.0       0.0       0.0
$---+----1----+----2----+----3----+----4----+----5----+----6----+----7-
---+----8
*BOUNDARY_SPC_NODE_ID
$       id
         1
$     node       cid      dofx      dofy      dofz     dofrx     dofry
dofrz
     97190         0         1         1         1         1         1
1
*BOUNDARY_SPC_NODE_ID
```

```
$       id
         2
$     node       cid      dofx      dofy      dofz     dofrx     dofry
dofrz
     97191         0         1         1         1         1         1
1
*BOUNDARY_SPC_NODE_ID
$       id
         3
$     node       cid      dofx      dofy      dofz     dofrx     dofry
dofrz
     97199         0         1         1         1         1         1
1
*BOUNDARY_SPC_NODE_ID
$       id
         4
$     node       cid      dofx      dofy      dofz     dofrx     dofry
dofrz
     97206         0         1         1         1         1         1
1
.
.
.
.

. $---+----1----+----2----+----3----+----4----+----5----+----6----+----
7----+----8
*INITIAL_VELOCITY_GENERATION
$CardName:BALL_VELOCITY
$       id      styp     omega        vx        vy        vz     ivatn
         5         2       0.0       0.0       0.0   -133.25         0
$       xc        yc        zc        nx        ny        nz     phase
       0.0       0.0       0.0       0.0       0.0       0.0         0
$---+----1----+----2----+----3----+----4----+----5----+----6----+----7-
---+----8
*CONTACT_AUTOMATIC_SURFACE_TO_SURFACE_ID
$       cid
          1BALL_WEFT
$     ssid      msid     sstyp     mstyp    sboxid    mboxid       spr
mpr
         5         2         3         3         0         0         0
0
$       fs        fd        dc        vc       vdc    penchk        bt
dt
       0.0       0.0       0.0       0.0       0.0         0       0.0
.1000E+21
$      sfs       sfm       sst       mst      sfst      sfmt       fsf
vsf
     1.000     1.000       0.0       0.0     1.000     1.000     1.000
1.000
$     soft    sofscl    lcidab    maxpar     sbopt     depth     bsort
frcfrq
         2   0.10000         0     1.025       0.0         2        10
1
$   penmax    thkopt    shlthk     snlog      isym     i2d3d    sldthk
sldstf
       0.0         0         0         0         0         0       0.0
0.0
$     igap    ignore    dprfac    dtstif     blank     blank    flangl
         1         0       0.0       0.0                           0.0
*CONTACT_AUTOMATIC_SURFACE_TO_SURFACE_ID
```

```
$      cid
         2BALL_WARF
$     ssid      msid     sstyp     mstyp    sboxid    mboxid       spr
mpr
         5         1         3         3         0         0         0
0
$       fs        fd        dc        vc       vdc    penchk        bt
dt
       0.0       0.0       0.0       0.0       0.0         0       0.0
.1000E+21
$      sfs       sfm       sst       mst      sfst      sfmt       fsf
vsf
     1.000     1.000       0.0       0.0     1.000     1.000     1.000
1.000
$     soft    sofscl    lcidab    maxpar     sbopt     depth     bsort
frcfrq
         2   0.10000         0     1.025       0.0         2        10
1
$   penmax    thkopt    shlthk     snlog      isym     i2d3d    sldthk
sldstf
       0.0         0         0         0         0         0       0.0
0.0
$     igap    ignore    dprfac    dtstif     blank     blank    flangl
         1         0       0.0       0.0                           0.0
*CONTACT_AUTOMATIC_SURFACE_TO_SURFACE_ID
$      cid
         3BALL_NANOFIBER
$     ssid      msid     sstyp     mstyp    sboxid    mboxid       spr
mpr
         5         3         3         3         0         0         0
0
$       fs        fd        dc        vc       vdc    penchk        bt
dt
       0.0       0.0       0.0       0.0       0.0         0       0.0
.1000E+21
$      sfs       sfm       sst       mst      sfst      sfmt       fsf
vsf
     1.000     1.000       0.0       0.0     1.000     1.000     1.000
1.000
$     soft    sofscl    lcidab    maxpar     sbopt     depth     bsort
frcfrq
         2   0.10000         0     1.025       0.0         2        10
1
$   penmax    thkopt    shlthk     snlog      isym     i2d3d    sldthk
sldstf
       0.0         0         0         0         0         0       0.0
0.0
$     igap    ignore    dprfac    dtstif     blank     blank    flangl
         1         0       0.0       0.0                           0.0
$---+----1----+----2----+----3----+----4----+----5----+----6----+----7-
---+----8
$---+----1----+----2----+----3----+----4----+----5----+----6----+----7-
---+----8
*NODE
$    nid               x               y               z      tc
rc
    2001 3.162848473E+00 3.000000238E+00 2.817026377E-01
    2002 3.164637804E+00 3.000000000E+00 3.929424286E-01
    2003 3.249682903E+00 3.000000000E+00 3.379999697E-01
    2004 3.153027534E+00 3.055697680E+00 2.817026377E-01
    2005 3.154708862E+00 3.056309462E+00 3.929424286E-01
```

```
    2006 3.234625101E+00 3.085396528E+00 3.379999697E-01
    2007 3.124749184E+00 3.104677200E+00 2.817026377E-01
    2008 3.126119852E+00 3.105827093E+00 3.929424286E-01
    2009 3.191268206E+00 3.160492897E+00 3.379999697E-01
    2010 3.081424236E+00 3.141031027E+00 2.817026377E-01
    2011 3.082318783E+00 3.142580509E+00 3.929424286E-01
    2012 3.124841452E+00 3.216231585E+00 3.379999697E-01
    2013 3.028278351E+00 3.160374641E+00 2.817026377E-01
    2014 3.028589010E+00 3.162136555E+00 3.929424286E-01
    2015 3.043357134E+00 3.245889425E+00 3.379999697E-01
    2016 2.971721649E+00 3.160374641E+00 2.817026377E-01
    2017 2.971410990E+00 3.162136555E+00 3.929424286E-01
    2018 2.956643343E+00 3.245889425E+00 3.379999697E-01
    2019 2.918575764E+00 3.141031027E+00 2.817026377E-01
    2020 2.917681217E+00 3.142580509E+00 3.929424286E-01
    2021 2.875159025E+00 3.216231585E+00 3.379999697E-01.
.
.
.
523333       3  210564  210662  210664  210566  158123  158122  158139
158142
  523334       3  210566  210664  210666  210568  158142  158139
158140  158141
  523335       3  210568  210666  210668  210570  158141  158140
158157  158160
  523336       3  210570  210668  210670  210572  158160  158157
158158  158159
  523337       3  210572  210670  210672  210574  158159  158158
158175  158178
  523338       3  210574  210672  210674  210576  158178  158175
158176  158177
  523339       3  210576  210674  210676  210578  158177  158176
158193  158196
  523340       3  210578  210676  210678  210580  158196  158193
158194  158195
  523341       3  210580  210678  210680  210582  158195  158194
158211  158214
  523342       3  210582  210680  210682  210584  158214  158211
158212  158213
  523343       3  210584  210682  210684  210586  158213  158212
158229  158232
  523344       3  210586  210684  210686  210588  158232  158229
158230  158231
  523345       3  210588  210686  210688  210590  158231  158230
158247  158250
  523346       3  210590  210688  210690  210592  158250  158247
158248  158249
  523347       3  210592  210690  210692  210594  158249  158248
158265  158268
  523348       3  210594  210692  210694  210596  158268  158265
158266  158267
  523349       3  210596  210694  210696  210598  158267  158266
158283  158286
  523350       3  210598  210696  210698  210600  158286  158283
158284  158285
  523351       3  210600  210698  210700  210602  158285  158284
158301  158304
  523352       3  210602  210700  210702  210604  158304  158301
158302  158303
  523353       3  210604  210702  210704  210606  158303  158302
158319  158322
```

```
  523354       3  210606  210704  210706  210608  158322  158319
158320  158321
$---+----1----+----2----+----3----+----4----+----5----+----6----+----7-
---+----8
*END
```